Fundamentals of Duct Acoustics

Sjoerd W. Rienstra
Technische Universiteit Eindhoven

16 November 2015

Contents

1 Introduction

In a duct of constant cross section, with a medium and boundary conditions independent of the axial position, the wave equation for time-harmonic perturbations may be solved by means of a series expansion in a particular family of self-similar solutions, called modes. They are related to the eigensolutions of a two-dimensional operator, that results from the wave equation, on a cross section of the duct. For the common situation of a uniform medium without flow, this operator is the well-known Laplace operator ∇^2. For a non-uniform medium, and in particular with mean flow, the details become more complicated, but the concept of duct modes remains by and large the same[1].

Modes are interesting mathematically because they form, in general, a complete basis by which any solution can be represented. Physically, modes are interesting because they are solutions in their own right – not just mathematical building blocks – and by their simple structure the usually complicated behaviour of the total field is more easily understood.

The concept of mode can be formulated rather generally. We have modes in ducts of arbitrary cross section, with any boundary condition and medium, with or without mean flow, as long as medium and boundary condition are constant in axial direction. The arbitrary cross section, with uniform medium and hard walls, is considered in section 2. However, to obtain insight *and* because it is a technically relevant configuration it is useful to simplify the mean flow and the geometry of the duct to a cylinder, and obtain modes of simpler shape. A hierarchy of equations from general to uniform and no mean flow are derived in section 3.1. We will consider only two of these, but the derivation of the others are included for useful reference.

The impedance boundary condition, including the physically necessary conditions and the refraction effects through a boundary layer, are given in section 3.2.

The hard-wall and soft-wall modes, with and without mean flow, in cylindrical ducts are discussed in the sections 4.1, 4.3, 5.1 and 5.2.

In section 6 some applications are given, including the sound field due to a point source found by means of Fourier transformation. This example is interesting because it shows how modes may appear naturally as residues of poles of the Fourier transformed solution, and not, for that matter, just by assuming solutions of a certain form.

In an other section the application of modes in reflection and transmission problems is discussed. In particular the important technique of mode-matching, which converts a complicated acoustic scattering problem in a relatively easy problem of linear algebra.

In the appendix, sections on Bessel functions, an important complex square root, and Myers' acoustic energy equations are included.

[1] Duct modes should not be confused with cavity modes. Cavity modes are solutions of the wave equation in a closed cavity that exist without forcing, and are related to resonance. They exist only for particular (resonance) frequencies. Duct modes, on the other hand exist for any given frequency.

Take for example a hard-walled box of sides a, b and c. Then solutions exist of the wave equation of the following form

$$\phi(\boldsymbol{x},t) = \cos\Big(\frac{\pi n x}{a}\Big)\cos\Big(\frac{\pi m y}{b}\Big)\cos\Big(\frac{\pi l z}{c}\Big)\,\mathrm{e}^{\mathrm{i}\omega t} \quad \text{if} \quad \frac{\omega}{c_0} = \pi\Big(\frac{n^2}{a^2}+\frac{m^2}{b^2}+\frac{l^2}{c^2}\Big)^{\frac{1}{2}}$$

yielding resonance frequencies ω_{mnl}.

2 General Formulation

The time-harmonic sound field p in a duct of constant cross section with linear boundary conditions that are independent of the axial coordinate x may be described by an infinite sum of special solutions, called modes, that retain their shape when travelling down the duct. With given frequency ω and the usual complex notation they are of the form

$$p(\boldsymbol{x},t) = \psi(y,z)f(x-vt) = \psi(y,z)\,\mathrm{e}^{\mathrm{i}\omega(t-\frac{x}{v})} = \psi(y,z)\,\mathrm{e}^{\mathrm{i}\omega t-\mathrm{i}kx} \tag{1}$$

and consist of an exponential function multiplied by a shape function ψ, being an eigenfunction of a Laplace-type operator valid on a duct cross section. The eigenfunction ψ corresponds to an eigenvalue that on its turn relates to axial wave number k.

In general, the set $\{\psi_n, k_n\}$ of shape function/wave number combinations is infinite and countable. From linearity they can be used as basis (building blocks) to construct more general solutions of the equations. Without mean flow or with uniform mean flow, the set of modes is rich enough to represent all solutions. This is almost, but not exactly, the case with non-uniform mean flow, where $\omega - ku_0$, referred to in (26, 32, 35), may be zero for a continuum of values of k (Brambley et al., 2012), and some solutions cannot be described by discrete modes.

In the present section we will elaborate this idea for the simple case of a hard-walled duct of arbitrary cross section with a uniform medium without mean flow. It is by far not exhaustive and primarily meant for illustration to see the cylindrical ducts, to be considered later, in perspective.

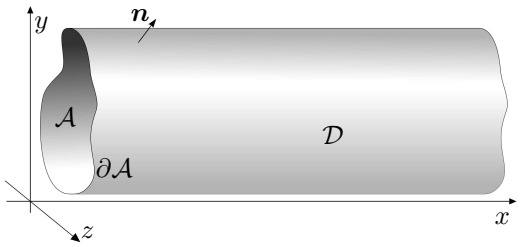

Figure 1: A duct $\mathcal{D}$ of cross section $\mathcal{A}$.

Consider the two-dimensional (simply connected) area $\mathcal{A}$ with a smooth boundary $\partial\mathcal{A}$ and an externally directed unit normal $\boldsymbol{n}$. When we consider, for definiteness, this area be part of the y,z-plane, it describes the duct $\mathcal{D}$ (see figure 1) by

$$\mathcal{D} = \{(x,y,z) \mid (y,z) \in \mathcal{A}\} \tag{2}$$

with axial cross sections being copies of $\mathcal{A}$ and the normal vectors $\boldsymbol{n}$ the same for all x. In the usual complex notation (with $+\mathrm{i}\omega t$–sign convention with real frequency ω), the acoustic field

$$p(\boldsymbol{x},t) := p(\boldsymbol{x})\,\mathrm{e}^{\mathrm{i}\omega t}, \quad \boldsymbol{v}(\boldsymbol{x},t) := \boldsymbol{v}(\boldsymbol{x})\,\mathrm{e}^{\mathrm{i}\omega t} \tag{3}$$

satisfies in the duct ($\boldsymbol{x} \in \mathcal{D}$) the equations

$$\nabla^2 p + \frac{\omega^2}{c_0^2}p = 0, \quad \mathrm{i}\omega\rho_0\boldsymbol{v} + \nabla p = 0. \tag{4}$$

Solutions of a more general time-dependence may be constructed via Fourier synthesis in ω, but here we will consider modes of a fixed, positive, frequency. At the duct wall we assume hard-wall boundary conditions

$$\boldsymbol{v} \cdot \boldsymbol{n} = 0 \quad \text{for} \quad \boldsymbol{x} \in \partial\mathcal{D} \tag{5}$$

but other locally reacting wall types (impedance walls) would make little difference. Self-similar solutions of the form $p(x, y, z) = \phi(x)\psi(y, z)$ exist for $\phi(x) = \mathrm{e}^{-\mathrm{i}kx}$ with particular values of k and associated functions ψ (determined up to a multiplicative factor). We thus have (with the exponential divided out)

$$\nabla^2_{yz}\psi + \Big(\frac{\omega^2}{c_0^2} - k^2\Big)\psi = 0, \tag{6}$$

where ∇^2_{yz} denotes the Laplacian ∇^2 in y and z, but since ψ is a function of y and z only, it makes no difference to write ∇^2 instead.

This leads to general solutions given by

$$p(x, y, z) = \sum_{n=0}^{\infty} C_n \psi_n(y, z)\, \mathrm{e}^{-\mathrm{i}k_n x} \tag{7}$$

where ψ_n are the eigenfunctions of the Laplace operator reduced to $\mathcal{A}$, i.e. solutions of

$$-\nabla^2\psi = \alpha^2\psi \quad \text{for} \quad (y, z) \in \mathcal{A}, \quad \text{with} \quad \nabla\psi \cdot \boldsymbol{n} = 0 \quad \text{for} \quad (y, z) \in \partial\mathcal{A}, \tag{8}$$

and α^2 is the corresponding eigenvalue. For the present hard wall boundary condition, the

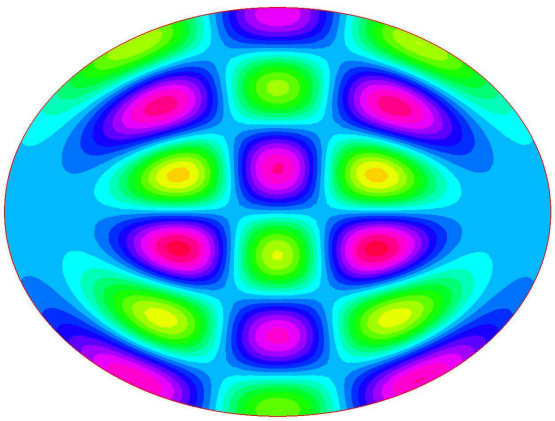

Figure 2: Example of modal shape function in an elliptic duct.

eigenvalues α_n^2 form a real and non-negative countable sequence, which starts with $\alpha_1^2 = 0$ and $\psi_1 = 1$. For a more general condition, like an impedance, they will be complex.

The axial wave number k is given by one of the square roots (+ for right and − for left running waves)

$$k_n^{\pm} = \pm\sqrt{\frac{\omega^2}{c_0^2} - \alpha_n^2} = \pm\frac{\omega}{c_0}\zeta\Big(\frac{\alpha_n c_0}{\omega}\Big) \tag{9}$$

where ζ is a carefully defined complex square root (Appendix A.2) that ensures the correct signs for any real or complex k. Each term in the series expansion, i.e. $\psi_n(y,z)\,\mathrm{e}^{-\mathrm{i}k_n x}$, is called a *duct mode*.

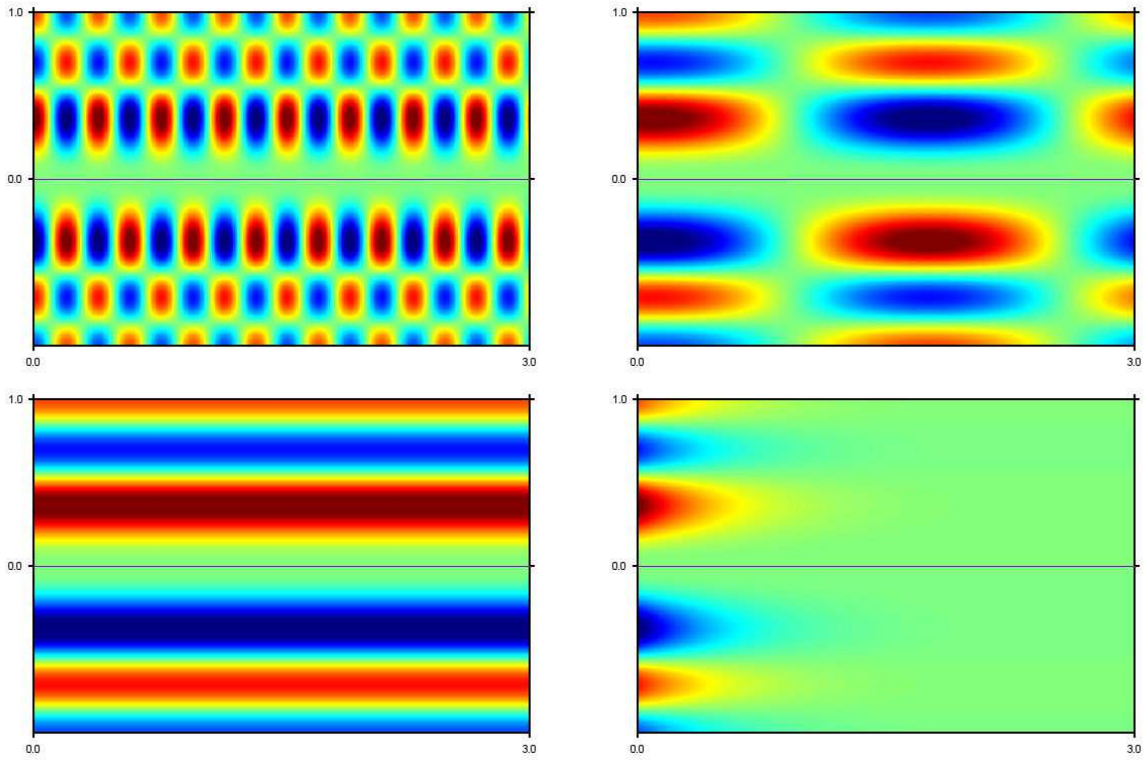

Figure 3: Axial patterns of modes with large, small, zero and imaginary k_n.

An important hallmark of a mode is the axial wavenumber k_n. If ω/c_0 is well above eigenvalue α_n, k_n is real and not small, and the axial modal behaviour is sinusoidal with an axial wave length which is not large (figure 3a). If the ω/c_0 is reduced to approach α_n, k_n becomes small and the axial wavelength large (figure 3b). If $\omega/c_0 = \alpha_n$ and $k_n = 0$, the mode is at resonance and the axial wave length is infinite (figure 3c). If $\omega/c_0 < \alpha_n$ and k_n is imaginary, the mode is exponentially decaying (figure 3d), or "cut off".

If the duct cross section is circular or rectangular and the boundary condition is uniform along the circumference, the symmetry of the geometry allows a symmetric modal shape function, and the solutions of the eigenvalue problem may be found by separation of variables. For example in a rectangular duct

$$\psi(y,z) = f(y)g(z)$$

the eigensolutions consist of combinations of trigonometric functions. In a circular duct in polar coordinates r, θ

$$\psi(y,z) = f(\theta)g(r)$$

these eigensolutions consist of exponentials in θ and Bessel functions in r.

Some other geometries, like ellipses, do also allow explicit solutions, but only in special cases such as with hard walls. For other geometries one has to fall back on numerical methods for the eigenvalue problem.

By application of Green's theorem it can easily be shown that the eigenfunctions $\{\psi_n\}$ are orthogonal to themselves.

If $n \neq m$ we have

$$\iint_{\mathcal{A}} \left[\psi_m(\nabla^2\psi_n + \alpha_n^2\psi_n) - \psi_n(\nabla^2\psi_m + \alpha_m^2\psi_m)\right] \mathrm{d}\sigma = (\alpha_n^2 - \alpha_m^2) \iint_{\mathcal{A}} \psi_n\psi_m \,\mathrm{d}\sigma = 0$$

If $n = m$ we have

$$\iint_{\mathcal{A}} \left[\psi_n\nabla^2\psi_n + \alpha_n^2\psi_n^2\right] \mathrm{d}\sigma = \alpha_n^2 \iint_{\mathcal{A}} \psi_n^2 \,\mathrm{d}\sigma - \iint_{\mathcal{A}} |\nabla\psi_n|^2 \,\mathrm{d}\sigma = 0 \tag{10}$$

It follows, that any $\alpha_n \neq 0$ can only be an eigenvalue if $\iint_{\mathcal{A}} \psi_n^2 \,\mathrm{d}\sigma \neq 0$. If $\alpha_0 = 0$, it is indeed an eigenvalue with solution $\psi_0 = 1$ and $\iint_{\mathcal{A}} \psi_0^2 \,\mathrm{d}\sigma = |\mathcal{A}| \neq 0$. Up to a factor it is the only solution because $\iint_{\mathcal{A}} |\nabla\psi_0|^2 \,\mathrm{d}\sigma = 0$ only if $|\nabla\psi_0| \equiv 0$.

Altogether we have thus

$$\iint_{\mathcal{A}} \psi_n^2 \,\mathrm{d}\sigma \begin{cases} = 0 & \text{if} \quad n \neq m \\ \neq 0 & \text{if} \quad n = m \end{cases} \tag{11}$$

Some care is required when, due to a symmetric geometry, each α_n is linked to more than one ψ_n. Note that for other boundary conditions, like impedances, ψ and α are in general complex valued. Although these integral relations remain the same, we cannot call the modes orthogonal to themselves, because for complex ψ the inner product is $\iint_{\mathcal{A}} \psi_n\overline{\psi_m} \,\mathrm{d}\sigma$.

Nevertheless, this orthogonality for hard walls is very useful to obtain the amplitudes of the modal expansion. See section 6.

In the next section we derive the major equations that result for sound in a parallel mean flow, i.e. a flow, constant in x direction. The no-flow and uniform flow cases will subsequently be considered in further detail.

As a final remark, we note that the above solution only needs a minor adaptation to include a uniform mean flow inside the duct.

3 The Equations

3.1 A Hierarchy of Equations

We start (Goldstein, 1976; Rienstra and Hirschberg, 2015; Oppeneer et al., 2016) from the fundamental law of thermodynamics for a reversible processes, in temperature T, entropy s, internal energy e, pressure p and density ρ,

$$T\mathrm{d}s = \mathrm{d}e + p\mathrm{d}(\rho^{-1}) \tag{12}$$

and the assumption of an ideal gas

$$p = \rho RT \tag{13}$$

with gas constant $R = C_p - C_v$ and heat capacities C_p and C_p. More in particular for a perfect gas with constant heat capacities and

$$e = C_v T = \frac{C_v p}{R\rho} \tag{14}$$

it follows that

$$T\mathrm{d}s = \mathrm{d}e + p\mathrm{d}(\rho^{-1}) = \frac{C_v}{\rho R}\mathrm{d}p + \left(\frac{C_v}{R} + 1\right) p\mathrm{d}(\rho^{-1}) = \frac{C_v}{\rho R}\mathrm{d}p - \frac{C_p p}{\rho^2 R}\mathrm{d}\rho$$

or

$$\mathrm{d}s = \frac{C_v}{p}\mathrm{d}p - \frac{C_p}{\rho}\mathrm{d}\rho$$

If we define the sound speed c by c^2 being the coefficient of isentropic variations of p with ρ, we obtain

$$c^2 = \left(\frac{\partial p}{\partial \rho}\right)_s = \frac{C_p p}{C_v \rho} = \gamma\frac{p}{\rho} \tag{15}$$

and so

$$\mathrm{d}s = \frac{C_v}{p}\left(\mathrm{d}p - c^2\mathrm{d}\rho\right)$$

The isentropic Euler equations, with velocity $\boldsymbol{v}$, position $\boldsymbol{x}$ and time t, are

$$\frac{\mathrm{d}\rho}{\mathrm{d}t} + \rho\nabla\cdot\boldsymbol{v} = 0, \quad \rho\frac{\mathrm{d}\boldsymbol{v}}{\mathrm{d}t} + \nabla p = 0, \quad \frac{\mathrm{d}s}{\mathrm{d}t} = 0 \tag{16}$$

while the isentropic relation of (16) reduces to

$$\frac{\mathrm{d}p}{\mathrm{d}t} = c^2\frac{\mathrm{d}\rho}{\mathrm{d}t} \tag{17}$$

When we write

$$\boldsymbol{v} = \boldsymbol{v}_0 + \boldsymbol{v}', \quad p = p_0 + p', \quad \rho = \rho_0 + \rho', \tag{18}$$

and linearize for small perturbations, we obtain for the mean flow

$$\nabla\cdot(\rho_0\boldsymbol{v}_0) = 0,\ \rho_0(\boldsymbol{v}_0\cdot\nabla)\boldsymbol{v}_0 + \nabla p_0 = 0,\ (\boldsymbol{v}_0\cdot\nabla)p_0 = c_0^2(\boldsymbol{v}_0\cdot\nabla)\rho_0,\ \gamma p_0 = \rho_0 c_0^2 \tag{19}$$

and the perturbations

$$\begin{aligned}
\frac{\partial \rho'}{\partial t} + \nabla\cdot(\boldsymbol{v}_0\rho' + \boldsymbol{v}'\rho_0) &= 0 \\
\rho_0\Big(\frac{\partial}{\partial t} + \boldsymbol{v}_0\cdot\nabla\Big)\boldsymbol{v}' + \rho_0\big(\boldsymbol{v}'\cdot\nabla\big)\boldsymbol{v}_0 + \rho'(\boldsymbol{v}_0\cdot\nabla)\boldsymbol{v}_0 + \nabla p' &= 0 \qquad (20)\\
\frac{\partial p'}{\partial t} + \boldsymbol{v}_0\cdot\nabla p' + \boldsymbol{v}'\cdot\nabla p_0 = c_0^2\Big(\frac{\partial \rho'}{\partial t} + \boldsymbol{v}_0\cdot\nabla\rho' + \boldsymbol{v}'\cdot\nabla\rho_0\Big) &+ c_0^2\big(\boldsymbol{v}_0\cdot\nabla\rho_0\big)\Big(\frac{p'}{p_0} - \frac{\rho'}{\rho_0}\Big).
\end{aligned}$$

If p_0 is constant, then $\boldsymbol{v}_0\cdot\nabla\boldsymbol{v}_0 = \boldsymbol{v}_0\cdot\nabla\rho_0 = 0$, and this last equation (20c) reduces to

$$\frac{\partial p'}{\partial t} + \boldsymbol{v}_0\cdot\nabla p' = c_0^2\left(\frac{\partial \rho'}{\partial t} + \boldsymbol{v}_0\cdot\nabla\rho' + \boldsymbol{v}'\cdot\nabla\rho_0\right)$$

If the mean flow is a parallel flow in x direction

$$\boldsymbol{v}_0 = u_0(y,z)\boldsymbol{e}_x, \quad \rho_0 = \rho_0(y,z), \quad c_0 = c_0(y,z), \qquad (21)$$

the equations (19) are satsified and we obtain, with $D_0 = \frac{\partial}{\partial t} + u_0\frac{\partial}{\partial x}$,

$$D_0\rho' + \rho_0\nabla\cdot\boldsymbol{v}' + v'\frac{\partial\rho_0}{\partial y} + w'\frac{\partial\rho_0}{\partial z} = 0 \qquad (22a)$$

$$\rho_0 D_0\boldsymbol{v}' + \rho_0\left(v'\frac{\partial u_0}{\partial y} + w'\frac{\partial u_0}{\partial z}\right)\boldsymbol{e}_x + \nabla p' = 0 \qquad (22b)$$

$$D_0 p' - c_0^2 D_0\rho' - c_0^2\left(v'\frac{\partial\rho_0}{\partial y} + w'\frac{\partial\rho_0}{\partial z}\right) = 0 \qquad (22c)$$

Since ρ_0 is independent of x, equation (22c) can be written as

$$c_0^2(\boldsymbol{v}'\cdot\nabla\rho_0) = D_0 p' - c_0^2 D_0\rho'$$

The convective derivative of the divergence of the momentum equation (22b)

$$D_0^2\left(\rho_0\nabla\cdot\boldsymbol{v}' + v'\frac{\partial\rho_0}{\partial y} + w'\frac{\partial\rho_0}{\partial z}\right) + 2\frac{\partial}{\partial x}\left(\rho_0 D_0 v'\frac{\partial u_0}{\partial y} + \rho_0 D_0 w'\frac{\partial u_0}{\partial z}\right) + D_0\nabla^2 p' = 0$$

becomes with the mass equation (22a) and again momentum equation (22b)

$$c_0^2 D_0^3\rho' + 2c_0^2\frac{\partial}{\partial x}\left(\frac{\partial p'}{\partial y}\frac{\partial u_0}{\partial y} + \frac{\partial p'}{\partial z}\frac{\partial u_0}{\partial z}\right) - D_0(c_0^2\nabla^2 p') = 0 \qquad (23)$$

Since $\rho_0 c_0^2$ is constant, we can write

$$\rho_0 c_0^2\nabla^2 p' = \nabla\cdot(\rho_0 c_0^2\nabla p') = \rho_0\nabla\cdot(c_0^2\nabla p') + c_0^2\nabla p'\cdot\nabla\rho_0$$

and so with the momentum equation (and using the fact that ρ_0 is independent of x)

$$\rho_0 c_0^2\nabla^2 p' = \rho_0\nabla\cdot(c_0^2\nabla p') - c_0^2\left(\rho_0 D_0\boldsymbol{v}'\cdot\nabla\rho_0\right)$$

or

$$c_0^2\nabla^2 p' = \nabla\cdot(c_0^2\nabla p') - D_0^2 p' + c_0^2 D_0^2\rho'$$

Noting the fact that u_0 is independent of x, equation (23) is then

$$D_0^3 p' - D_0 \nabla\cdot(c_0^2 \nabla p') + 2c_0^2 \frac{\partial}{\partial x}(\nabla p' \cdot \nabla u_0) = 0. \tag{24}$$

This is the most general wave equation in the pressure for linear acoustic (i.e. isentropic) perturbations of a *parallel inviscid* mean flow with *uniform* (constant) mean pressure p_0. The corresponding velocity is to be found from (for example) equation (22b).

Starting from this general equation, we can further simplify to harmonic perturbations and more in particular modes in x direction. If the perturbations are harmonic in time, like $\propto \mathrm{e}^{\mathrm{i}\omega t}$, then we have the slight simplification $D_0 = \mathrm{i}\omega + u_0 \frac{\partial}{\partial x}$. A more important simplification is obtained if (in addition to the mean flow) the boundary conditions are independent of x, in such a way that we can Fourier transform to x, or (which is more or less the same) assume the existence of solutions (modes) of the form

$$p'(\boldsymbol{x}, t) = \mathrm{Re}\big(\hat{p}(y,z)\,\mathrm{e}^{\mathrm{i}\omega t - \mathrm{i}kx}\big), \quad \boldsymbol{v}'(\boldsymbol{x}, t) = \mathrm{Re}\big(\hat{\boldsymbol{v}}(y,z)\,\mathrm{e}^{\mathrm{i}\omega t - \mathrm{i}kx}\big), \tag{25}$$

for certain wave number k. Then we have the significant simplification

$$\boxed{\begin{aligned} \Omega^2 \nabla\cdot\Big(\frac{c_0^2}{\Omega^2}\nabla\hat{p}\Big) + \big(\Omega^2 - k^2 c_0^2\big)\hat{p} &= 0, \quad \text{with} \quad \Omega = \omega - k u_0, \\ \rho_0 \Omega \hat{u} + \frac{\nabla\hat{p}\cdot\nabla u_0}{\Omega} - k\hat{p} &= 0 \\ \rho_0 \Omega \hat{v} - \mathrm{i}\frac{\partial \hat{p}}{\partial y} &= 0 \\ \rho_0 \Omega \hat{w} - \mathrm{i}\frac{\partial \hat{p}}{\partial z} &= 0 \end{aligned}} \tag{26}$$

Equation (26a) is the most general equation to describe modes. It is a partial differential equation in y and z (the ∇-operator only relates to y and z), where together with $\hat{p}$ also finding the possible values of k are now part of the problem. Equations (26b, 26c, 26d) express the perturbation velocity in terms of $\hat{p}$. We can further simplify as follows.

If the mean flow is uniform, with $u_0 = U_\infty$ constant, then $\Omega = \Omega_\infty$ is constant and[2]

$$\begin{aligned} \nabla\cdot\big(c_0^2\nabla\hat{p}\big) + \big(\Omega_\infty^2 - k^2 c_0^2\big)\hat{p} &= 0 \\ \rho_0 \Omega_\infty \hat{u} - k\hat{p} &= 0 \\ \rho_0 \Omega_\infty \hat{v} - \mathrm{i}\frac{\partial \hat{p}}{\partial y} &= 0 \\ \rho_0 \Omega_\infty \hat{w} - \mathrm{i}\frac{\partial \hat{p}}{\partial z} &= 0 \end{aligned} \tag{27}$$

With uniform mean flow and a uniform medium c_0 constant, we have a form of the

[2]It may be noted that the seemingly trivial solution $p \equiv 0$ is not without meaning. It corresponds with convective incompressible pressureless disturbance with $\Omega_\infty = 0$ of the form $\boldsymbol{v} \propto \exp\big(-\mathrm{i}\frac{\omega}{U_\infty}x\big)$

Helmholtz equation in $\hat{p}$

$$\begin{aligned} \nabla^2\hat{p} + \Big(\frac{\Omega_\infty^2}{c_0^2} - k^2\Big)\hat{p} &= 0 \\ \rho_0\Omega_\infty\hat{u} - k\hat{p} &= 0 \\ \rho_0\Omega_\infty\hat{v} - \mathrm{i}\frac{\partial\hat{p}}{\partial y} &= 0 \\ \rho_0\Omega_\infty\hat{w} - \mathrm{i}\frac{\partial\hat{p}}{\partial z} &= 0 \end{aligned} \tag{28}$$

Without mean flow, with $u_0 = 0$, we have

$$\begin{aligned} \nabla\cdot\big(c_0^2\nabla\hat{p}\big) + \big(\omega^2 - k^2c_0^2\big)\hat{p} &= 0 \\ \rho_0\omega\hat{u} - k\hat{p} &= 0 \\ \rho_0\omega\hat{v} - \mathrm{i}\frac{\partial\hat{p}}{\partial y} &= 0 \\ \rho_0\omega\hat{w} - \mathrm{i}\frac{\partial\hat{p}}{\partial z} &= 0 \end{aligned} \tag{29}$$

If the medium is uniform, with c_0 constant, we have a form of the **Helmholtz equation**

$$\boxed{\begin{aligned} \nabla^2\hat{p} + \Big(\frac{\omega^2}{c_0^2} - k^2\Big)\hat{p} &= 0 \\ \rho_0\omega\hat{u} - k\hat{p} &= 0 \\ \rho_0\omega\hat{v} - \mathrm{i}\frac{\partial\hat{p}}{\partial y} &= 0 \\ \rho_0\omega\hat{w} - \mathrm{i}\frac{\partial\hat{p}}{\partial z} &= 0 \end{aligned}} \tag{30}$$

If c_0 and u_0 only depend on y and we can assume solutions of the form

$$p'(\boldsymbol{x},t) = \mathrm{Re}\big(\hat{p}(y)\,\mathrm{e}^{\mathrm{i}\omega t - \mathrm{i}kx - \mathrm{i}\nu z}\big), \quad \boldsymbol{v}'(\boldsymbol{x},t) = \mathrm{Re}\big(\hat{\boldsymbol{v}}(y)\,\mathrm{e}^{\mathrm{i}\omega t - \mathrm{i}kx - \mathrm{i}\nu z}\big) \tag{31}$$

then (26a) becomes the **2D Pridmore-Brown equation**, with corresponding equations for the velocity

$$\boxed{\begin{aligned} \frac{\Omega^2}{c_0^2}\Big(\frac{c_0^2}{\Omega^2}\hat{p}'\Big)' + \Big(\frac{\Omega^2}{c_0^2} - k^2 - \nu^2\Big)\hat{p} &= 0 \\ \rho_0\Omega\hat{u} + \frac{\hat{p}'u_0'}{\Omega} - k\hat{p} &= 0 \\ \rho_0\Omega\hat{v} - \mathrm{i}\hat{p}' &= 0 \\ \rho_0\Omega\hat{w} - \nu\hat{p} &= 0 \end{aligned}} \tag{32}$$

where the prime denotes a derivative to y. The equation simplifies to a form of the

harmonic equation if c_0 and u_0 are constant

$$\begin{aligned} \hat{p}'' + \Big(\frac{\Omega_\infty^2}{c_0^2} - k^2 - \nu^2\Big)\hat{p} &= 0 \\ \rho_0\Omega_\infty\hat{u} - k\hat{p} &= 0 \\ \rho_0\Omega_\infty\hat{v} - \mathrm{i}\hat{p}' &= 0 \\ \rho_0\Omega_\infty\hat{w} - \nu\hat{p} &= 0 \end{aligned} \tag{33}$$

If the medium is circularly symmetric with $u_0 = u_0(r)$ and $c_0 = c_0(r)$ in polar coordinates (x, r, θ) while $\boldsymbol{v} = u\boldsymbol{e}_x + v\boldsymbol{e}_r + w\boldsymbol{e}_\theta$ and $\nabla = \boldsymbol{e}_x\frac{\partial}{\partial x} + \boldsymbol{e}_r\frac{\partial}{\partial r} + \boldsymbol{e}_\infty\frac{1}{r}\frac{\partial}{\partial\theta}$, and we can assume solutions of the form

$$p'(\boldsymbol{x}, t) = \mathrm{Re}\big(\hat{p}(r)\,\mathrm{e}^{\mathrm{i}\omega t - \mathrm{i}kx - \mathrm{i}m\theta}\big), \quad \boldsymbol{v}'(\boldsymbol{x}, t) = \mathrm{Re}\big(\hat{\boldsymbol{v}}(r)\,\mathrm{e}^{\mathrm{i}\omega t - \mathrm{i}kx - \mathrm{i}m\theta}\big) \tag{34}$$

then (26a) becomes the **3D Pridmore-Brown equation**, with corresponding equations for the velocity

$$\boxed{\begin{aligned} \frac{\Omega^2}{rc_0^2}\Big(\frac{rc_0^2}{\Omega^2}\hat{p}'\Big)' + \Big(\frac{\Omega^2}{c_0^2} - k^2 - \frac{m^2}{r^2}\Big)\hat{p} &= 0 \\ \rho_0\Omega\hat{u} + \frac{\hat{p}'u_0'}{\Omega} - k\hat{p} &= 0 \\ \rho_0\Omega\hat{v} - \mathrm{i}\hat{p}' &= 0 \\ \rho_0\Omega\hat{w} - \frac{m}{r}\hat{p} &= 0 \end{aligned}} \tag{35}$$

where the prime denote a derivative to r. If c_0 and u_0 are constant this reduces to a form of **Bessel's equation** (Appendix A.1)

$$\boxed{\begin{aligned} \hat{p}'' + \frac{1}{r}\hat{p}' + \Big(\frac{\Omega_\infty^2}{c_0^2} - k^2 - \frac{m^2}{r^2}\Big)\hat{p} &= 0 \\ \rho_0\Omega_\infty\hat{u} - k\hat{p} &= 0 \\ \rho_0\Omega_\infty\hat{v} - \mathrm{i}\hat{p}' &= 0 \\ \rho_0\Omega_\infty\hat{w} - \frac{m}{r}\hat{p} &= 0 \end{aligned}} \tag{36}$$

Without mean flow this is obviously

$$\boxed{\begin{aligned} \hat{p}'' + \frac{1}{r}\hat{p}' + \Big(\frac{\omega^2}{c_0^2} - k^2 - \frac{m^2}{r^2}\Big)\hat{p} &= 0 \\ \rho_0\omega\hat{u} - k\hat{p} &= 0 \\ \rho_0\omega\hat{v} - \mathrm{i}\hat{p}' &= 0 \\ \rho_0\omega\hat{w} - \frac{m}{r}\hat{p} &= 0 \end{aligned}} \tag{37}$$

3.2 Boundary Conditions. Impedance.

We will consider ducts with hard walls, or soft walls of impedance type. Porous walls with bulk reacting material or flexible walls, allowing waves propagating in and along the wall, are outside the scope of the present introduction.

The boundary condition of a hard wall is simple. The wall is closed for any flow, so the normal component[3] of the acoustic velocity vanishes

$$\boldsymbol{v}' \cdot \boldsymbol{n} = 0, \quad \boldsymbol{x} \in \text{wall}, \quad \boldsymbol{n} \perp \text{wall}. \tag{38}$$

The boundary condition for an impedance wall is formulated in terms of the time Fourier transformed acoustic pressure and normal velocity. The Fourier transform is defined by

$$\hat{p}(\boldsymbol{x},\omega) = \frac{1}{2\pi}\int_{-\infty}^{\infty} p'(\boldsymbol{x},t)\,\mathrm{e}^{-\mathrm{i}\omega t}\,\mathrm{d}t, \quad p'(\boldsymbol{x},t) = \int_{-\infty}^{\infty} \hat{p}(\boldsymbol{x},\omega)\,\mathrm{e}^{\mathrm{i}\omega t}\,\mathrm{d}\omega. \tag{39}$$

The ratio of $\hat{p}$ and $\hat{\boldsymbol{v}}\cdot\boldsymbol{n}$ is equal to the wall impedance Z as follows

$$\hat{p} = Z\big(\hat{\boldsymbol{v}}\cdot\boldsymbol{n}\big), \quad \boldsymbol{x} \in \text{wall}. \tag{40}$$

$Z(\omega)$ is, to be physically possible, essentially depending on frequency. By convention the normal vector $\boldsymbol{n}$ is pointing *into* the wall, as the wall *impedes* the acoustic pressure. Z may depend on position $\boldsymbol{x}$, but for modes to exist, it is here assumed uniform.

For a problem with fixed frequency we can choose any Z, but in time domain more is required. First we observe that the equation turns into a convolution product like

$$p'(\boldsymbol{x},t) = \frac{1}{2\pi}\int_{-\infty}^{\infty} z(t-\tau)v'(\boldsymbol{x},\tau)\,\mathrm{d}\tau, \quad v'(\boldsymbol{x},t) = \frac{1}{2\pi}\int_{-\infty}^{\infty} y(t-\tau)p'(\boldsymbol{x},\tau)\,\mathrm{d}\tau \tag{41}$$

with $\boldsymbol{x} \in$ wall, $v' = \boldsymbol{v}'\cdot\boldsymbol{n}$, and

$$z(t) = \int_{-\infty}^{\infty} Z(\omega)\,\mathrm{e}^{\mathrm{i}\omega t}\,\mathrm{d}\omega, \quad y(t) = \int_{-\infty}^{\infty} Z(\omega)^{-1}\,\mathrm{e}^{\mathrm{i}\omega t}\,\mathrm{d}\omega \tag{42}$$

Necessary conditions for Z follow then from basic physical arguments (Rienstra, 2006).

(i) **Reality** (the original field variables are real), $Z(\omega) = \overline{Z(-\omega)}$;

(ii) **Passivity** (the wall only absorbs energy), $\mathrm{Re}(Z) \geqslant 0$ for all ω;

(iii) **Causality** ($\hat{p}$ and $\hat{\boldsymbol{v}}$ cannot predict each other's future), which usually amounts, with $\mathrm{e}^{\mathrm{i}\omega t}$ convention and Z sufficiently well behaved[4] at infinity, to $Z(\omega)$ being *free of zeros and poles* in the *lower complex half plane* $\mathrm{Im}(\omega) < 0$.

[3] The tangential component does not have to be zero since the flow model is inviscid.

[4] This condition depends on the assumed notion of Fourier transforms. Integrability of Z in the classic sense is sufficient, but usually too strict. If we allow the inverse Fourier transform $z(t)$ to be a generalised function, with algebraic behaviour of $Z(\omega)$ for $\omega \to \infty$, we can include, for example, $Z(\omega) = R$ a constant, with $z(t) = 2\pi R\delta(t)$ which is perfectly causal.

A common example is the impedance of mass-spring-damper type

$$Z(\omega) = R + \mathrm{i}\omega m - \frac{\mathrm{i}K}{\omega} \tag{43}$$

with $R, m, K \geqslant 0$ and the pole in $\omega = 0$ assumed to belong to the upper half plane.

The above impedance condition is valid with a mean flow velocity vanishing at the wall. With an inviscid flow model, the mean flow velocity along the wall may be non-zero. Although this is a modelling assumption and in reality we have a vanishingly thin boundary layer (vortex sheet), the acoustic pressure and velocity we are dealing with are *not* really at the wall, but at the top of the boundary layer, just inside the mean flow.

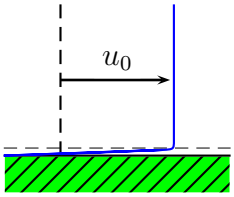

Figure 4: The thin boundary layer limit results in the Ingard/Ingard-Myers condition

In this situation we have to incorporate the refraction effects of the (vanishingly thin) boundary layer into the boundary condition. This may be done by introducing the perturbed wall streamline as intermediary, to obtain Ingard's condition (Ingard, 1959)

$$\Big(\mathrm{i}\omega + u_0\frac{\partial}{\partial x}\Big)\hat{p} = \mathrm{i}\omega Z\big(\hat{\boldsymbol{v}}\cdot\boldsymbol{n}\big), \quad \boldsymbol{x} \in \text{wall} \tag{44}$$

valid for mean flow in x direction. The more general situation of flow along an arbitrarily curved surface, due to Myers (1980), is more complicated

$$\Big(\mathrm{i}\omega + \boldsymbol{v}_0\cdot\nabla - \boldsymbol{n}\cdot\big(\boldsymbol{n}\cdot\nabla\big)\Big)\hat{p} = \mathrm{i}\omega Z\big(\hat{\boldsymbol{v}}\cdot\boldsymbol{n}\big), \quad \boldsymbol{x} \in \text{wall} \tag{45}$$

We will not use this condition here in the setting of straight ducts.

Finally, it should be noted that a *very thin* boundary layer along an impedance wall may be unstable for certain (complex) frequencies, leading in time domain to an absolute instability (an instability that is not convected away with the mean flow but grows exponentially at any point of observation). More in particular, the growth rate becomes infinite for a *vanishing* boundary layer, leading to an ill-posed, unphysical, problem in time domain (Brambley, 2009). A regularised boundary condition should be used, for example by allowing for a very thin, but non-zero boundary layer thickness (Rienstra and Darau, 2011).

In frequency domain, however, there is no problem. We are free to prescribe the frequency of interest, and if this is real, the worst instability we may have to deal with is a convective instability. The only problem is perhaps the fact that this instability is very sensitive to the boundary layer thickness (Rienstra and Vilenski, 2008), and may not be predicted accurately by a vanishing boundary layer model.

3.3 Non-dimensionalisation

Since we don't want to get lost in a jungle of symbols and variables, it is wise to make our problem dimensionless.

Consider in a duct, with radius a, wall impedance Z, uniform sound speed c_0, mean flow velocity U_∞ and mean density ρ_0, time-harmonic acoustic waves of angular frequency ω and modal wave number k. We scale our variables as follows

$$\begin{aligned} &\boldsymbol{x} := a\boldsymbol{x}, \quad t := \frac{at}{c_0}, \quad \hat{p} := \rho_0 c_0^2 p, \quad \hat{\rho} := \rho_0 \rho, \quad \hat{\boldsymbol{v}} := c_0 \boldsymbol{v}, \\ &\omega := \frac{\omega c_0}{a}, \qquad k := \frac{k}{a}, \qquad Z := \rho_0 c_0 Z, \qquad U_\infty := c_0 M, \end{aligned} \tag{46}$$

while intensity scales on $\rho_0 c_0^3$ and power on $\rho_0 c_0^3 a^2$. The impedance Z is usually scaled on the *local* density and sound speed, but since we consider here only uniform mean flows, this is equivalent to ρ_0 and c_0. M is known as the mean flow Mach number.

Note that we used for notational convenience the same symbol for the dimensional and dimensionless frequency ω. If ω is the dimensional frequency, then $k_0 = \omega/c_0$ is the corresponding free field wave number. The dimensionless quantity

$$He = \frac{\omega a}{c_0} = k_0 a \tag{47}$$

is called the **Helmholtz number**, and the most important parameter in duct acoustics. It is just equal to our dimensionless frequency ω.

4 Uniform Medium, No Mean Flow

4.1 Hard-walled Cylindrical Ducts

With a uniform medium, a circular duct and no mean flow, we have the equations (37), which become in dimensionless form

$$\begin{aligned} p'' + \frac{1}{r}p' + \Big(\omega^2 - k^2 - \frac{m^2}{r^2}\Big)p &= 0 \\ \omega u - kp &= 0 \\ \omega v - \mathrm{i}p' &= 0 \\ \omega w - \frac{m}{r}p &= 0 \end{aligned} \tag{48}$$

With hard walls, the boundary condition at $r = 1$ is then a vanishing radial velocity v, which implies

$$\frac{\partial p}{\partial r} = 0 \tag{49}$$

At $r = 0$ we assume a regular behaviour, since the singularity in the equations is not physical, but only due to the polar coordinate system. Furthermore, the field is clearly periodic in θ.

The solutions that result are then integer values for m, and Bessel functions (see Appendix A.1) for p

$$p(r) = J_m(\alpha_{m\mu} r) \tag{50}$$

The radial and axial modal wave numbers $\alpha_{m\mu}$ and $k_{m\mu}$ are related by a dispersion relation

$$\alpha_{m\mu}^2 + k_{m\mu}^2 = \omega^2 \tag{51}$$

yielding for given $\alpha_{m\mu}$ the left and right running wave numbers $k = k_{m\mu}^{\pm}$

$$k_{m\mu}^{+} = \sqrt{\omega^2 - \alpha_{m\mu}^2}, \quad k_{m\mu}^{-} = -\sqrt{\omega^2 - \alpha_{m\mu}^2} \tag{52}$$

where the square root is defined by $k_{m\mu}^{\pm} = \pm\omega\zeta(\alpha_{m\mu}/\omega)$ of Appendix A.2.

The radial modal wave numbers $\alpha_{m\mu}$ follow from the boundary condition

$$J_m'(\alpha_{m\mu}) = 0 \tag{53}$$

and are therefore just equal to the non-trivial positive zero's $j_{m\mu}'$ of J_m'. This means that only $\alpha_{01} = 0$ and all the others are strictly positive.

Since these zero's form an ever increasing sequence of positive real numbers, the axial wave numbers are either real or imaginary. From the definition it follows that $\mathrm{Re}(k_{m\mu}^{+}) \geqslant 0$, $\mathrm{Im}(k_{m\mu}^{+}) \leqslant 0$, $\mathrm{Re}(k_{m\mu}^{-}) \leqslant 0$, $\mathrm{Im}(k_{m\mu}^{-}) \geqslant 0$.

The associated solutions of the wave equation

$$J_m(\alpha_{m\mu} r)\, \mathrm{e}^{\mathrm{i}\omega t - \mathrm{i}m\theta - \mathrm{i}k_{m\mu}^{\pm} x} \tag{54}$$

are called duct modes, and they form a complete set of building blocks suitable for constructing any sound field in a duct. At the same time, they are particular shape-preserving solutions with easily interpretable properties.

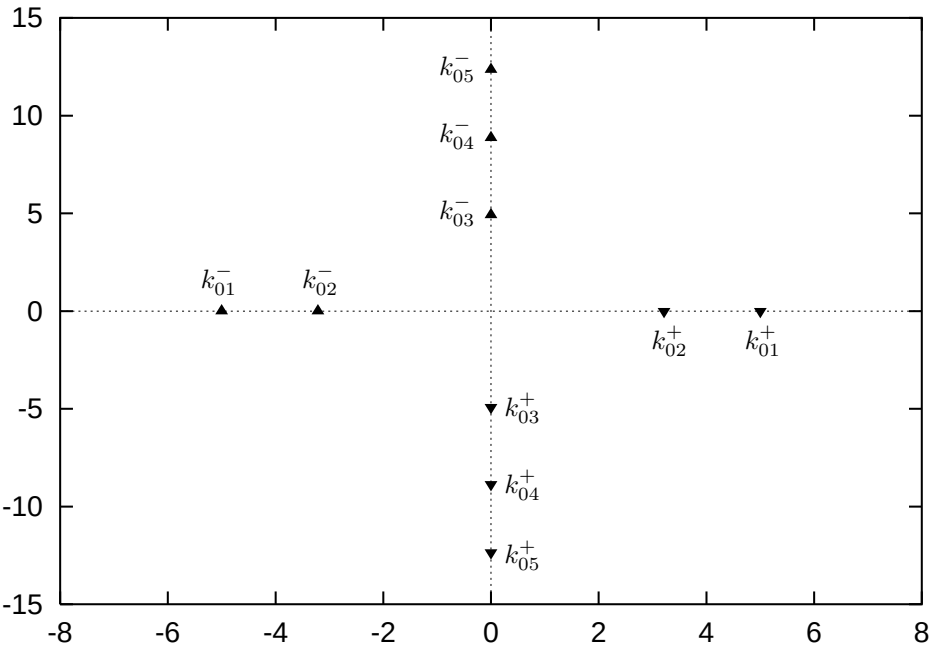

Figure 5: Complex axial wave numbers ($m = 0$, $\omega = 5$).

All $\alpha_{m\mu}$ and m are real, while only a finite number of $k_{m\mu}^{\pm}$ are real; see figure 5. The branch we selected here of the complex square root in $k_{m\mu}^{\pm}$ is chosen such that $\mathrm{e}^{-\mathrm{i}k_{m\mu}^{+}x}$ describes a right-running wave and $\mathrm{e}^{-\mathrm{i}k_{m\mu}^{-}x}$ a left-running wave. This will be further clarified later.

If we normalise the modes in a convenient way, by using (142), such that

$$\int_0^1 N_{m\mu}^2 J(\alpha_{m\mu} r)^2 \, r \, \mathrm{d}r = 1 \tag{55}$$

and neglect the $\mathrm{e}^{\mathrm{i}\omega t}$ factor, we obtain

$$U_{m\mu}(r)\, \mathrm{e}^{-\mathrm{i}m\vartheta - \mathrm{i}k_{m\mu}^{\pm}x},\ U_{m\mu}(r) = N_{m\mu} J_m(\alpha_{m\mu} r),\ N_{m\mu} = \frac{\sqrt{2}}{J_m(\alpha_{m\mu})\sqrt{1 - \dfrac{m^2}{\alpha_{m\mu}^2}}}, \tag{56}$$

except that $N_{01} = \sqrt{2}$. They form (for fixed x) a complete set (in L_2-norm over (r, ϑ)), so by superposition we can write any harmonic solution as the following modal expansion in pressure and axial velocity

$$p(x, r, \vartheta) = \sum_{m=-\infty}^{\infty} \sum_{\mu=1}^{\infty} (A_{m\mu}\, \mathrm{e}^{-\mathrm{i}k_{m\mu}^{+}x} + B_{m\mu}\, \mathrm{e}^{-\mathrm{i}k_{m\mu}^{-}x}) U_{m\mu}(r)\, \mathrm{e}^{-\mathrm{i}m\vartheta}, \tag{57a}$$

$$u(x, r, \vartheta) = \frac{1}{\omega} \sum_{m=-\infty}^{\infty} \sum_{\mu=1}^{\infty} (k_{m\mu}^{+} A_{m\mu}\, \mathrm{e}^{-\mathrm{i}k_{m\mu}^{+}x} + k_{m\mu}^{-} B_{m\mu}\, \mathrm{e}^{-\mathrm{i}k_{m\mu}^{-}x}) U_{m\mu}(r)\, \mathrm{e}^{-\mathrm{i}m\vartheta}\,. \tag{57b}$$

The normalisation factor $N_{m\mu}$ is chosen such that a modal amplitude $A_{m\mu}$ scales with the energy content of the corresponding mode (see below).

A surface of constant phase, $m\vartheta + \mathrm{Re}(k^{\pm}_{m\mu})x = \text{constant}$, is a helicoid of pitch $2\pi m/|\mathrm{Re}(k^{\pm}_{m\mu}|)$; see figure 6.

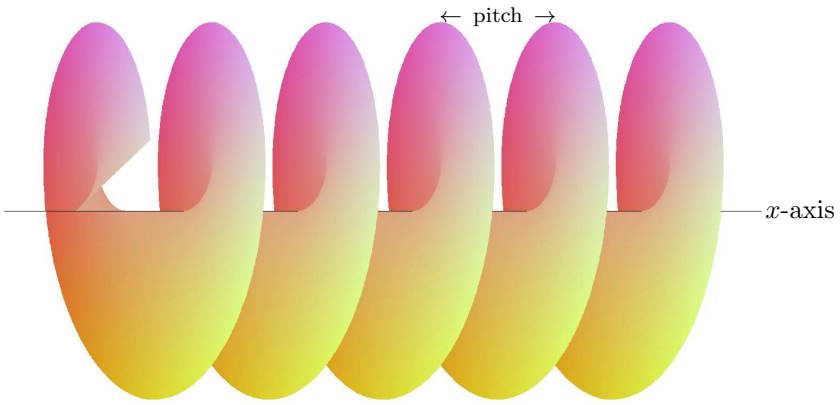

Figure 6: Surface of constant phase $m\vartheta + \mathrm{Re}(k^{\pm}_{m\mu})x$.

An important special case is the plane wave $m = 0$, $\mu = 1$, with

$$j'_{01} = 0, \quad \alpha_{01} = 0, \quad k^{\pm}_{01} = \pm\omega, \quad N_{01} = \sqrt{2}, \quad p^{\pm}_{01} = \sqrt{2}\,\mathrm{e}^{\mp \mathrm{i}\omega x}\,. \tag{58}$$

In fact, this is the only non-trivial eigenvalue equal to zero. All others are greater, the smallest being given by

$$j'_{11} = 1.84118\cdots\,. \tag{59}$$

Since the zeros of J'_m form an ever increasing sequence both in m and in μ (with $j'_{m\mu} \simeq (\mu + \frac{1}{2}m - \frac{3}{4})\pi$ for $\mu \to \infty$; see Appendix A.1), there are for any ω always a (finite) $\mu = \mu_0$ and $m = m_0$ beyond which $\alpha^2_{m\mu} > \omega^2$, so that $k_{m\mu}$ is purely imaginary, and the mode decays exponentially in x.

So we see that there are always a *finite* number of modes with *real* $k_{m\mu}$ (see figure 5). Since they are the only modes that propagate (see below), they are called *cut-on*. The remaining infinite number of modes, with *imaginary* $k_{m\mu}$, are evanescent and therefore called *cut-off*.

For low frequency, i.e. for

$$\omega < j'_{11} = 1.84118\cdots \tag{60}$$

all modes are cut-off except for the plane wave. In this case a plane wave approximation (i.e. considering only the first mode) is applicable if we are far enough away from any sources, changes in boundary condition, or other scattering objects, for the generated evanescent modes to become negligible. In general we say that a mode propagates or decays exponentially depending on the frequency being lower or higher than the cut-off or resonance frequency

$$f_c = \frac{j'_{m\mu} c_0}{2\pi a}. \tag{61}$$

There are various ways to portray the modal wave numbers. Important and meaningful are the locations of $k^{\pm}_{m\mu}$ in the complex plane (figure 5). If they are real, the mode is

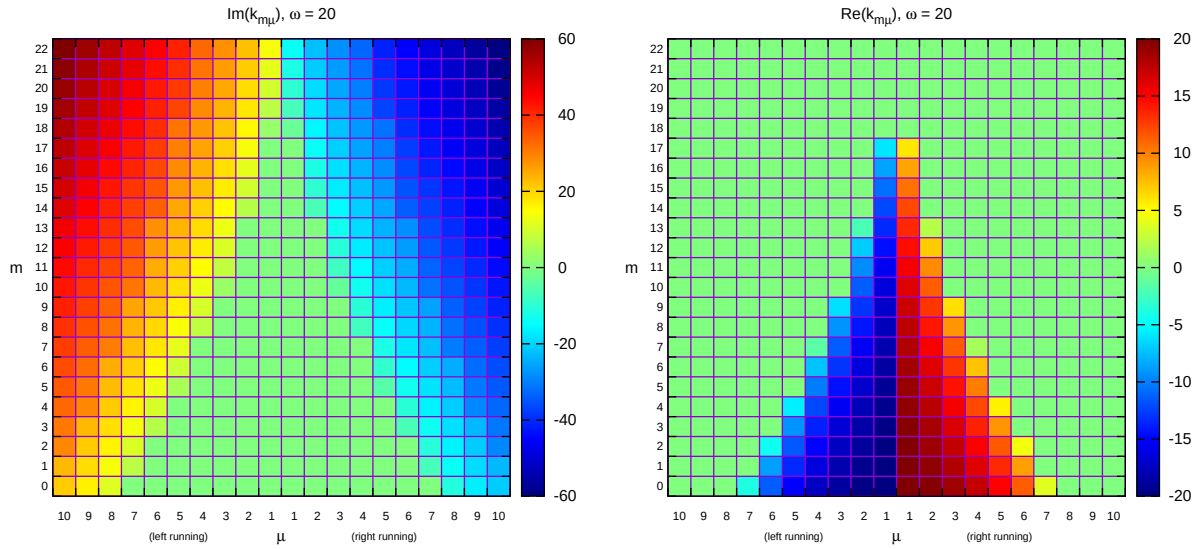

Figure 7: Imaginary and real parts of left and right running modal wave numbers

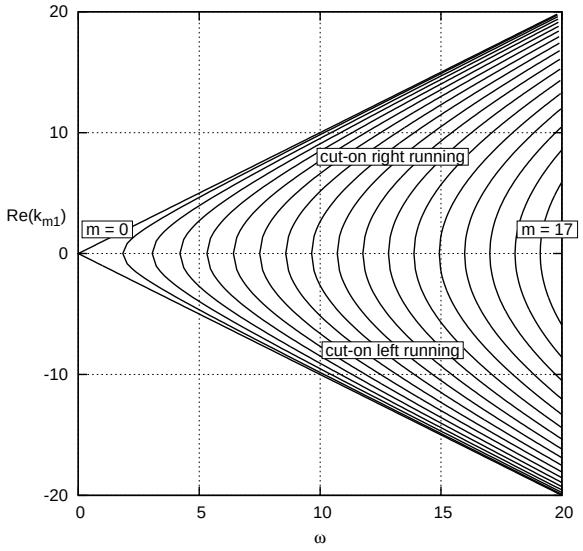

Figure 8: Real part of the 1st radial cut-on modes, as a function of Helmholtz number ω

cut-on and propagates without attenuation, while for any complex wave number, the corresponding mode decays according to

$$\propto \mathrm{e}^{\mathrm{Im}(k^{\pm}_{m\mu})x} \quad \text{for } x \to \pm\infty \tag{62}$$

Other graphical representations are figures 7 of $\mathrm{Im}\, k^{\pm}_{m\mu}$ and $\mathrm{Re}\, k^{\pm}_{m\mu}$ coloured for each index combination m, μ. The triangle where $\mathrm{Im}\, k_{m\mu} = 0$ (cut-on) is clearly visible. In figure 8 we see the first radial modes $\mathrm{Re}\, k_{m1}$ as a function of ω. We see indeed that each m-modes are cut-on only above a certain frequency.

By orthogonality relation[5] (11)

$$\int_0^1 \int_0^{2\pi} U_{m\mu}(r)\,\mathrm{e}^{-\mathrm{i}m\vartheta}\,\overline{\left(U_{n\nu}(r)\,\mathrm{e}^{-\mathrm{i}n\vartheta}\right)} r\,\mathrm{d}\vartheta\mathrm{d}r = 2\pi\delta_{mn}\delta_{\mu\nu} \tag{63}$$

we find by integration of the time-averaged axial intensity (146b)

$$\langle \boldsymbol{I}\cdot\boldsymbol{e}_x\rangle = \tfrac{1}{4}(p\overline{u}+\overline{p}u) = \tfrac{1}{2}\,\mathrm{Re}(p\overline{u}) \tag{64}$$

over a duct cross section $x =$ constant the transmitted acoustic power (148)

$$\mathcal{P} = \frac{\pi}{\omega}\sum_{m=-\infty}^{\infty}\sum_{\mu=1}^{\mu_0}\left(k^+_{m\mu}|A_{m\mu}|^2 + k^-_{m\mu}|B_{m\mu}|^2\right) + \frac{2\pi}{\omega}\sum_{m=-\infty}^{\infty}\sum_{\mu=\mu_0+1}^{\infty}\left(\tau_{m\mu}\,\mathrm{Im}(A_{m\mu}\overline{B_{m\mu}})\right). \tag{65}$$

where $\mu_0 = \mu_0(m)$ is the number of cut-on modes per m, and $\tau_{m\mu} = \mathrm{i}k^+_{m\mu} = -\mathrm{i}k^-_{m\mu}$ is positive real if $k^\pm_{m\mu}$ is imaginary. Note that $k^-_{m\mu} = -k^+_{m\mu}$.

With only right- or only left-running modes ($B_{m\mu} = 0$ or $A_{m\mu} = 0$), this summation consists of only a *finite* number of terms: the cut-on modes. In this situation only cut-on modes propagate energy. The distinction between "right" and "left" running modes is confirmed for cut-on modes by the direction of propagation of the energy. With only right-running modes the power $\mathcal{P} > 0$ is positive and clearly the energy propagates to the right, and with only left-running modes the power $\mathcal{P} < 0$ is negative and the energy propagates to the left (Morfey, 1971).

Cut-off modes decay in positive direction for right-running modes, and in negative direction for left-running modes. Left- or right-running cut-off modes alone do not propagate energy, but in combination they do, as is clear from the term with $A_{m\mu}\overline{B_{m\mu}}$ in (65). In this way it is possible that through a finite section of a duct with only cut-off modes, energy is transported from one end to the other. This is called "tunnelling".

The axial *phase velocity* (the velocity of a wave crest) of a cut-on mode is equal to

$$v_f^\pm = \frac{\omega}{k^\pm_{m\mu}} \tag{66}$$

The axial *group velocity* (the signal velocity) of a cut-on mode is given by

$$v_g^\pm = \left(\frac{\mathrm{d}k^\pm_{m\mu}}{\mathrm{d}\omega}\right)^{-1} = \frac{k^\pm_{m\mu}}{\omega}. \tag{67}$$

Note that $v_g = 0$ at the cut-off frequency, while for the other frequencies

$$v_g^\pm v_f^\pm = 1, \quad \text{with } \; v_f^- \leqslant -1 \leqslant v_g^- < 0 < v_g^+ \leqslant 1 \leqslant v_f^+ \tag{68}$$

Except for the plane 01−wave, where $v_f = v_g = \pm 1$, the axial group velocity is smaller than 1 (i.e. smaller than c_0 dimensionally) because the modal wave fronts do not propagate parallel to the x-axis, but rather follow a longer path. For $m \neq 0$ they spiral around the x-axis, with a right-hand rotation for $m > 0$ and a left-hand rotation for $m < 0$.

[5] $\delta_{ij} = 1$ if $i = j$, $\delta_{ij} = 0$ if $i \neq j$

4.2 Rectangular Ducts

In a completely analogous way as in the foregoing section 4.1, the general modal solution of equation (33) of sound propagation in a rectangular hard walled duct of sides a and b, can be found. We find the crosswise wave numbers α_n, β_m and axial wave numbers k_{nm}

$$\alpha_n = \frac{n\pi}{a}, \quad \beta_m = \frac{m\pi}{b}, \quad k_{nm}^{\pm} = \pm\sqrt{\omega^2 - \alpha_n^2 - \beta_m^2}, \tag{69}$$

where $n = 0, 1, 2, \ldots$ and $m = 0, 1, 2, \ldots$ and the definition of the square root follows again Appendix A.2. So the analogue of formula (57a), is then

$$p(x, y, z) = \sum_{n=0}^{\infty}\sum_{m=0}^{\infty} \cos(\alpha_n x)\cos(\beta_m y)(A_{nm}\,\mathrm{e}^{-\mathrm{i}k_{nm}^{+}z} + B_{nm}\,\mathrm{e}^{-\mathrm{i}k_{nm}^{-}z}). \tag{70}$$

4.3 Soft Wall Modes

When the duct is lined with sound absorbing material of a type that allows little or no sound propagation in the material parallel to the wall, the material is called *locally reacting* and may be described by a wall impedance $Z(\omega)$, giving the boundary condition (40) here as

$$\mathrm{i}\omega p = -Z\frac{\partial p}{\partial r} \quad \text{at} \quad r = 1. \tag{71}$$

A typical practical example is the inlet of an aircraft turbojet engine. The previous concept of a modal expansion, with modes again retaining their shape travelling down the duct, is also here applicable. The general solution has a form similar to (56) and (57a), the hard walled case. Only the eigenvalues $\alpha_{m\mu}$ are now defined by

$$\frac{J_m(\alpha_{m\mu})}{\alpha_{m\mu}J_m'(\alpha_{m\mu})} = \frac{\mathrm{i}Z}{\omega}, \tag{72}$$

related to $k_{m\mu}$ by the same square root (143) as before:

$$k_{m\mu}^{\pm} = \pm\sqrt{\omega^2 - \alpha_{m\mu}^2} = \pm\omega\zeta(\alpha_{m\mu}/\omega).$$

The soft-wall modes are *not* orthogonal, but a normalization that preserves the relation

$$\int_0^1 U_{m\mu}(r)\overline{U_{m\mu}(r)}r\,\mathrm{d}\vartheta\mathrm{d}r = 1$$

is

$$N_{m\mu} = \frac{|Z|}{|J_m(\alpha_{m\mu})|}\sqrt{\frac{\mathrm{Im}(\alpha_{m\mu}^2)}{\omega\,\mathrm{Re}(Z)}}. \tag{73}$$

Qualitatively, the behaviour of these modes in the complex $k_{m\mu}$-plane is as follows.

If $\mathrm{Im}(Z) > 0$, all modes may be found not very far from their hard wall values on the real interval $(-\omega, \omega)$ or the imaginary axis (that is, with $\alpha_{m\mu} = j'_{m\mu}$.) More precisely, if we vary Z from $|Z| = \infty$ to $Z = 0$, $\alpha_{m\mu}$ varies from its $|Z| = \infty$-value $j'_{m\mu}$ to its $Z = 0$-value $j_{m\mu}$. ($j_{m\mu}$ is the μ-th zero of J_m.) These $j_{m\mu}$ and $j'_{m\mu}$ are real and interlaced according to

the inequalities $j'_{m\mu} < j_{m\mu} < j_{m,\mu+1} <$ etc., so the corresponding $k_{m\mu}$ are also interlaced and shift into a direction of increasing mode number μ.

However, if $\mathrm{Im}(Z) < 0$ (for $+\mathrm{i}\omega t$-sign convention), a couple of two modes wander into their quarter of the complex plane in a more irregular way, and in general quite far away from the others. In figure 10 this behaviour is depicted by the trajectories of the modes as the impedance varies along lines of constant real part (figure 9). For small enough $\mathrm{Re}(Z)$

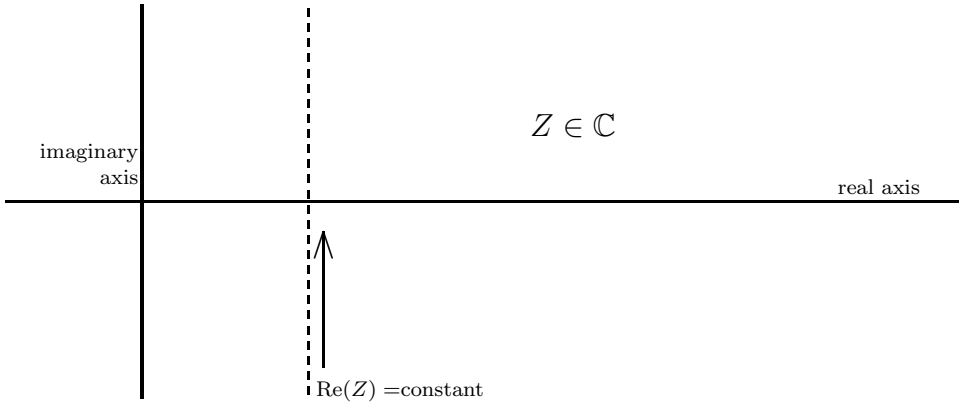

Figure 9: Trajectories in complex impedance plane for mode tracing.

(here, smaller than 1.4) we see the first (μ=1) mode being launched into the complex $k_{m\mu}$-plane when $\mathrm{Im}(Z)$ is negative, and then returning as a (for example) $\mu = 2$ or 4 mode when $\mathrm{Im}(Z)$ is positive. We will call these irregular modes *surface waves*: their maximum is at the wall surface, and away from the wall they decay exponentially (Rienstra, 2003). This is most purely the case for an imaginary impedance $Z = \mathrm{i}X$. See figure 11.

A solution $\alpha_{m\mu} = \mathrm{i}\,\varrho_{m\mu}$, $\varrho_{m\mu}$ real, may be found[6] satisfying

$$\frac{I_m(\varrho_{m\mu})}{\varrho_{m\mu} I'_m(\varrho_{m\mu})} = -\frac{X}{\omega} \qquad \text{if} \quad -\frac{\omega}{m} < X < 0. \tag{74}$$

The modal shape in r, described by $J_m(\alpha_{m\mu} r) = \mathrm{i}^m I_m(\varrho_{m\mu} r)$, is exponentially restricted to the immediate neighbourhood of $r = 1$ and indeed shows the surface wave character, since the modified Bessel function $I_m(x)$ has exponential behaviour for $x \to \infty$.

It is interesting to note that the corresponding axial wave number $|k^{\pm}_{m\mu}| = (\omega^2 + \varrho^2_{m\mu})^{1/2}$ ($k^{\pm}_{01}$ in figure 11) is now *larger* than ω. Hence, the modal phase velocity $\omega/|k^{\pm}_{m\mu}| < 1$, which amounts, dimensionally, to being smaller than the sound speed. This is indeed to be expected for a *non-radiating* surface wave.

Since the group velocity (67) depends on the way Z depends on ω, little can be said about it unless we know $Z(\omega)$.

[6]The function $h(z) = zI'_m(z)/I_m(z)$ increases monotonically, from $h(0) = m$ to $h(z) \sim z$ as $z \to \infty$.

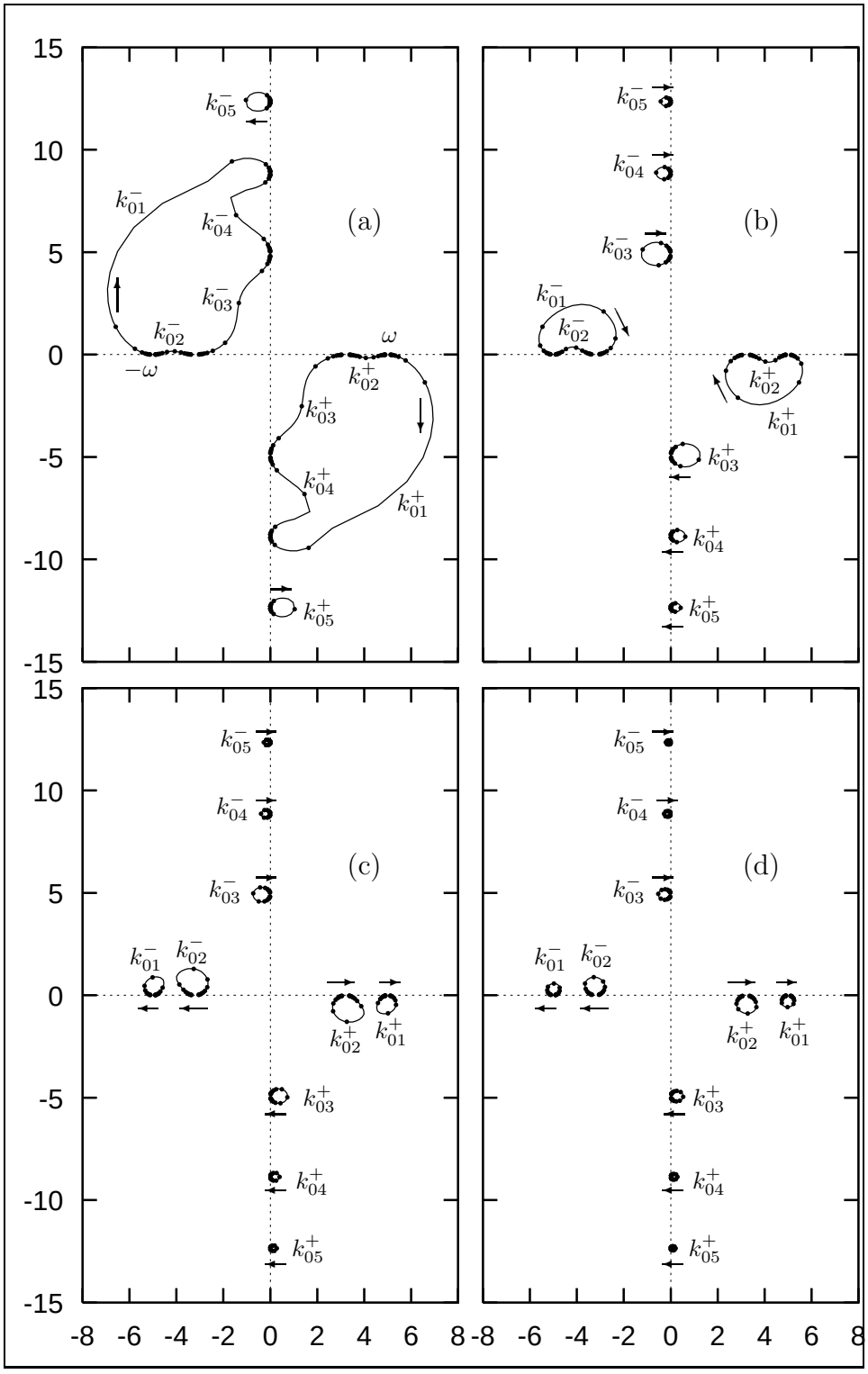

Figure 10: Trajectories of $k_{m\mu}$ ($m = 0$, $\omega = 5$) for $\mathrm{Im}(Z)$ varying from $-\infty$ to ∞ and fixed $\mathrm{Re}(Z)$ = (a) 0.5, (b) 1.0, (c) 1.5, (d) 2.0.

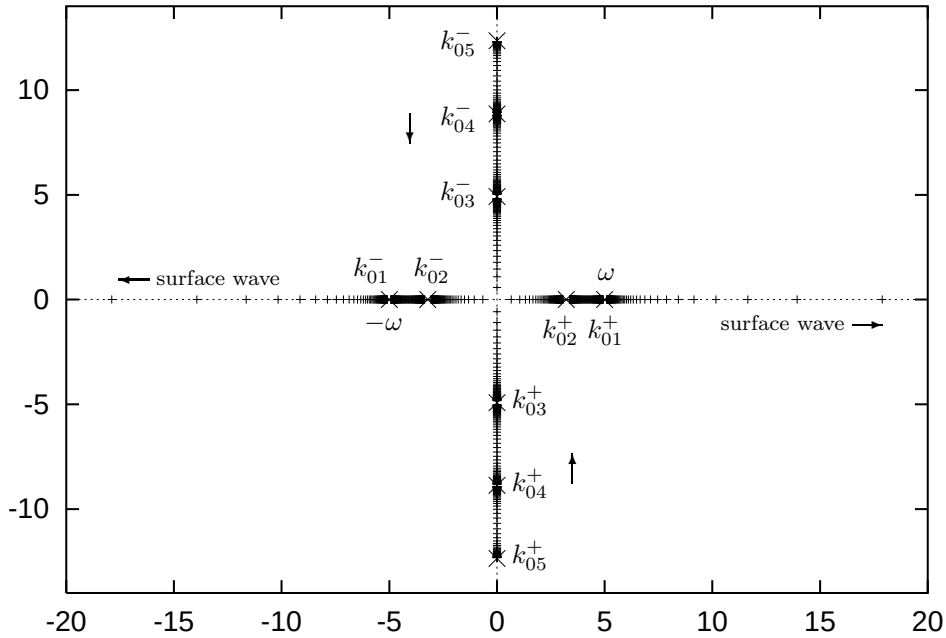

Figure 11: Trajectories of $k_{m\mu}^{\pm}$ ($m = 0$, $\omega = 5$) for $\mathrm{Im}(Z)$ varying from $-\infty$ to ∞ and fixed $\mathrm{Re}(Z) = 0$. $k_{0,n+1}^{\pm}$ become $k_{0,n}^{\pm}$. $k_{01}^{\pm}$ turn into surface waves.

4.4 Attenuation of Sound

Usually, lining is applied to reduce the sound level by dissipation. It is a simple exercise to verify that the time-averaged intensity at the wall directed into the wall (i.e. the dissipated power density) of a mode is

$$\langle \boldsymbol{I} \cdot \boldsymbol{e}_r \rangle \propto \mathrm{Im}(\alpha_{m\mu}^2). \tag{75}$$

A natural practical question is then: which impedance Z gives the greatest reduction. This question has, however, many answers. In general, the optimum will depend on the source of the sound. If more than one frequency contributes, we have to include the way $Z = Z(\omega)$ depends on ω. Also the geometry may play a rôle. Although it is strictly speaking not dissipation, the net reduction may benefit from reflections at discontinuities in the duct (hard/soft walls, varying cross section).

A simple approach would be to look at the reduction per mode, and to maximize the decay rate of the least attenuated mode, i.e. the one with the *smallest* $|\mathrm{Im}(k_{m\mu})|$. A further simplification is based on the observation that the decay rate $\mathrm{Im}(k_{m\mu})$ of a mode increases with increasing order, so that a (relatively) large decay rate is obtained if the first and second mode (of the most relevant m) *coalesce* (Cremer's optimum). This is obtained if also the derivative to $\alpha_{m\mu}$ of (72) vanishes, yielding the additional condition

$$J'_m(\alpha)^2 + \Big(1 - \frac{m^2}{\alpha^2}\Big) J_m(\alpha)^2 = 0 \tag{76}$$

An example is given in figure 12. No mode is lost, as the two corresponding modes degenerate into

$$\begin{aligned} J_m(\alpha_{m\mu} r) N_{m\mu}\, \mathrm{e}^{-\mathrm{i}k_{m\mu}x - \mathrm{i}m\vartheta}, \\ \Big(\alpha_{m\mu} x J_m(\alpha_{m\mu} r) - \mathrm{i}k_{m\mu} r J'_m(\alpha_{m\mu} r)\Big) N_{m\mu}\, \mathrm{e}^{-\mathrm{i}k_{m\mu}x - \mathrm{i}m\vartheta}. \end{aligned} \tag{77}$$

Equation (76) does not involve a problem parameter, so it can be solved for once, yielding

$$\alpha_0 = 2.98038 + 1.27960\mathrm{i},\ \alpha_1 = 4.46630 + 1.46747\mathrm{i},\ \alpha_2 = 5.81685 + 1.60001\mathrm{i},\ \ldots \quad (78)$$

(etc.) The corresponding constants $K_m = -\mathrm{i}J_m(\alpha_m)/\alpha_m J'_m(\alpha_m)$

$$K_0 = 0.28330 - 0.12163\mathrm{i},\ K_1 = 0.20487 - 0.07049\mathrm{i},\ K_2 = 0.16628 - 0.05133\mathrm{i},\ \ldots \quad (79)$$

lead to the relatively universal result (dimensionally) of optimal impedances

$$Z_m^{(opt)} = \rho_0 c_0 \frac{\omega a}{c_0} K_m, \quad (80)$$

scaling only linearly with the Helmholtz number (as indeed follows directly from (72)). Note that for more complicated geometries (like with a mean flow), the Cremer-optimal impedances cannot be given like this, as they depend on other problem parameters.

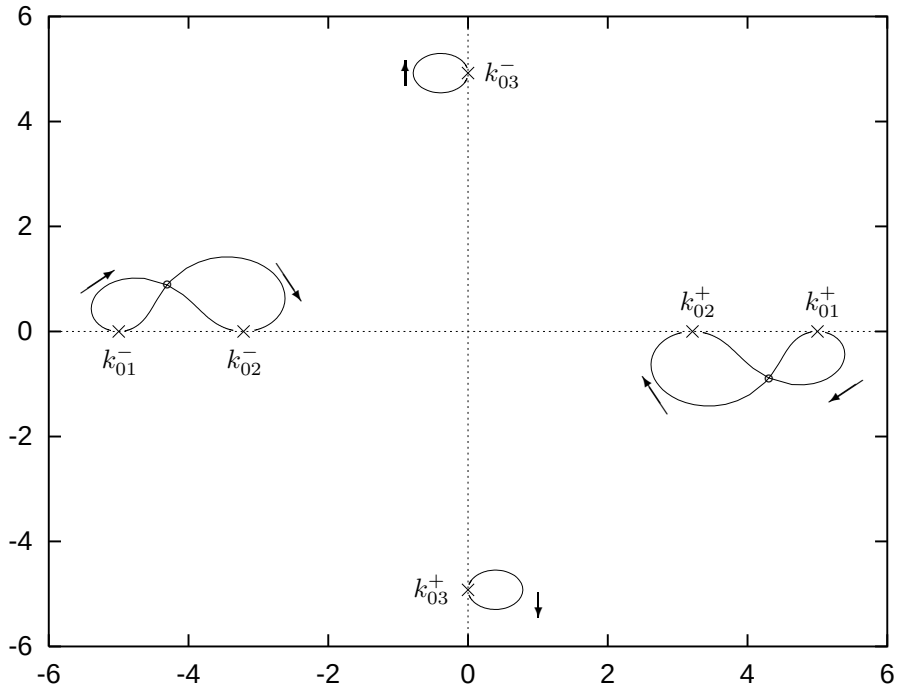

Figure 12: Trajectories of $k_{m\mu}^{\pm}$ ($m = 0$, $\omega = 5$) passing Cremer's optimum. Im(Z) varies from $-\infty$ to ∞ and Re(Z) is fixed at 1.4165. At $Z = 1.4165 - \mathrm{i}0.6082$ the first two modes coalesce as $k_{01}^{\pm} = k_{02}^{\pm} = \pm(4.3057, -0.8857)$.

5 Uniform Medium with Mean Flow

5.1 Hard-walled Cylindrical Ducts

The effects of mean flow are important. In general the equations (the Pridmore-Brown equation 35 and variants thereof) are difficult to analyse, but with uniform mean flow (36) we can work out the modal theory in great detail. We consider a hollow duct of (dimensionless) radius 1. We have then equation (36), which are in non-dimensional form

$$\begin{aligned} p'' + \frac{1}{r}p' + \Big((\omega - Mk)^2 - k^2 - \frac{m^2}{r^2}\Big)p = 0 \\ (\omega - Mk)u - kp = 0 \end{aligned} \tag{81}$$

Like before, the eigenvalue problem can now be solved, and we may expand the general solution (except for the pressureless convected perturbations) in Fourier-Bessel modes

$$p(x,r,\theta) = \sum_{m=-\infty}^{\infty}\sum_{\mu=1}^{\infty}\Big(A_{m\mu}\,\mathrm{e}^{-\mathrm{i}k^+_{m\mu}x} + B_{m\mu}\,\mathrm{e}^{-\mathrm{i}k^-_{m\mu}x}\Big)U_{m\mu}(r)\,\mathrm{e}^{-\mathrm{i}m\theta} \tag{82}$$

where the radial modes and radial and axial wave numbers satisfy

$$\begin{aligned} &U''_{m\mu} + \frac{1}{r}U'_{m\mu} + \Big(\alpha^2_{m\mu} - \frac{m^2}{r^2}\Big)U_{m\mu} = 0 \\ &\alpha^2_{m\mu} = (\omega - Mk_{m\mu})^2 - k^2_{m\mu} \\ &k^\pm_{m\mu} = \frac{-\omega M \pm \sqrt{\omega^2 - \beta^2\alpha^2_{m\mu}}}{\beta^2}, \qquad \beta = \sqrt{1-M^2} \end{aligned} \tag{83}$$

and solution (regular in $r = 0$)

$$U_{m\mu}(r) = N_{m\mu}J_m(\alpha_{m\mu}r). \tag{84}$$

In order to sort the right and left running modes we define the square root in $k_{m\mu}$ as before by using the square root (143) (see figures 13 and 14)

$$\sqrt{\omega^2 - \beta^2\alpha^2_{m\mu}} = \omega\zeta\left(\beta\frac{\alpha_{m\mu}}{\omega}\right). \tag{85}$$

The corresponding phase and group velocities for cut-on modes are found to be

$$v_f^\pm = \frac{\omega}{k^\pm_{m\mu}}, \tag{86}$$

$$v_g^\pm = \Big(\frac{\mathrm{d}k^\pm_{m\mu}}{\mathrm{d}\omega}\Big)^{-1} = \frac{k^\pm_{m\mu}}{\omega - Mk^\pm_{m\mu}} + M. \tag{87}$$

Note that $v_g = 0$ at the cut-off frequency, while for the other frequencies

$$(v_f^\pm - M)(v_g^\pm - M) = 1. \tag{88}$$

Due to the mean flow, the axial modal wave numbers are shifted to the left ($M > 0$), or right ($M < 0$), by a fixed amount of $-\omega M/\beta^2$, while the (dimensionless) cut-off frequency

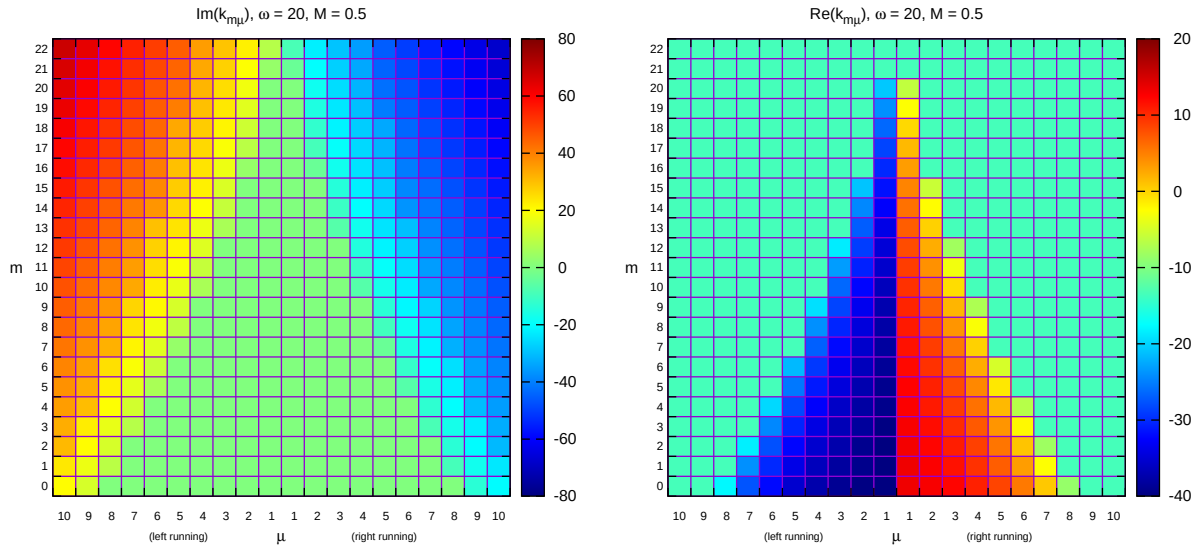

Figure 13: Imaginary and real parts of left and right running modal wave numbers

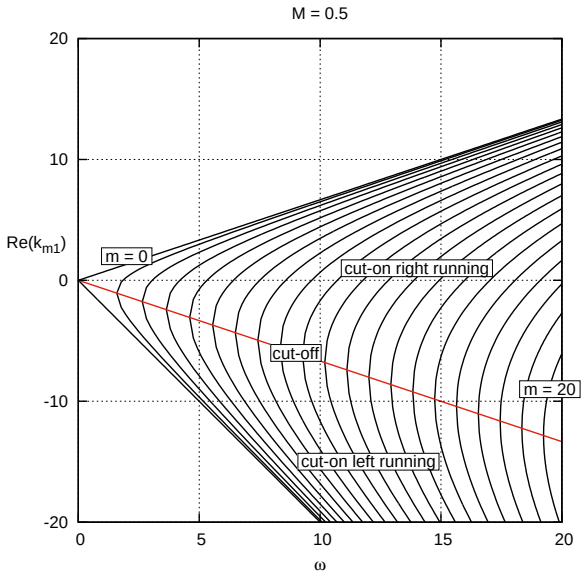

Figure 14: Real part of the 1st radial modes, as a function of Helmholtz number ω

is lowered from $\omega = \alpha_{m\mu}$ for no flow to $\omega = \beta\alpha_{m\mu}$ with flow. So with flow more modes are possibly cut-on than without. Note that (for $M > 0$) a right-running $m\mu-$mode for frequencies along the interval $\beta\alpha_{m\mu} < \omega < \alpha_{m\mu}$ has a *negative* phase velocity, which is thus *opposite* to its group velocity. Altogether we have for $M > 0$

$$\begin{aligned} v_f^- < M - 1 < v_g^- < 0 \quad & \text{on} \quad \beta\alpha_{m\mu} < \omega \\ v_f^+ < 0 < v_g^+ < M \quad & \text{on} \quad \beta\alpha_{m\mu} < \omega < \alpha_{m\mu} \\ 0 < M < v_g^+ < 1 + M < v_f^+ \quad & \text{on} \quad \alpha_{m\mu} < \omega \end{aligned} \tag{89}$$

Similar relations apply if $M < 0$. Since $v_g^- < 0 < v_g^+$, this shows that it is not the sign of $k_{m\mu}$ but of its radical that corresponds with the direction of propagation (c.f. eq. 95).

Eigenvalues $\alpha_{m\mu}$ are determined like before (53). Again, we normalise $U_{m\mu}$ like (56), while they are orthogonal and satisfy (63).

It is convenient to introduce the *Lorentz* or *Prandtl-Glauert* type transformation

$$x = \beta X, \quad \omega = \beta\Omega, \quad \alpha_{m\mu} = \Omega\gamma_{m\mu}, \quad k^{\pm}_{m\mu} = \frac{\Omega\sigma^{\pm}_{m\mu} - \Omega M}{\beta}, \quad \sigma^{\pm}_{m\mu} = \pm\sqrt{1-\gamma^2_{m\mu}} \tag{90}$$

where the sign of $\sigma^{\pm}_{m\mu}$ follows definition (143). Then we have for pressure p and axial acoustic velocity u

$$p = \sum_{m=-\infty}^{\infty}\sum_{\mu=1}^{\infty}\Big(A_{m\mu}\,\mathrm{e}^{-\mathrm{i}\Omega\sigma^{+}_{m\mu}X} + B_{m\mu}\,\mathrm{e}^{-\mathrm{i}\Omega\sigma^{-}_{m\mu}X}\Big)\,\mathrm{e}^{\mathrm{i}\Omega MX}\,U_{m\mu}(r)\,\mathrm{e}^{-\mathrm{i}m\theta} \tag{91}$$

$$u = \sum_{m=-\infty}^{\infty}\sum_{\mu=1}^{\infty}\Big(\frac{\sigma^{+}_{m\mu}-M}{1-M\sigma^{+}_{m\mu}}A_{m\mu}\,\mathrm{e}^{-\mathrm{i}\Omega\sigma^{+}_{m\mu}X} + \frac{\sigma^{-}_{m\mu}-M}{1-M\sigma^{-}_{m\mu}}B_{m\mu}\,\mathrm{e}^{-\mathrm{i}\Omega\sigma^{-}_{m\mu}X}\Big)\,\mathrm{e}^{\mathrm{i}\Omega MX}\,U_{m\mu}(r)\,\mathrm{e}^{-\mathrm{i}m\theta}$$

This includes the important case of the plane wave $m = 0$, $\mu = 1$, with $\alpha_{01} = 0$, $k^{\pm}_{01} = \pm\omega/(1 \pm M)$ and $U_{01} = \sqrt{2}$, such that

$$\begin{aligned} p(x,r,\theta) &= \sqrt{2}\Big(A_{01}\,\mathrm{e}^{-\frac{\mathrm{i}\omega x}{1+M}} + B_{01}\,\mathrm{e}^{\frac{\mathrm{i}\omega x}{1-M}}\Big) \\ u(x,r,\theta) &= \sqrt{2}\Big(A_{01}\,\mathrm{e}^{-\frac{\mathrm{i}\omega x}{1+M}} - B_{01}\,\mathrm{e}^{\frac{\mathrm{i}\omega x}{1-M}}\Big) \end{aligned} \tag{92}$$

If we have at position $x = 0$ a given pressure and axial velocity profiles $P(0,r,\theta)$ and $V(0,r,\theta)$, we can expand these profiles in the following Fourier-Bessel series

$$[P(0,r,\theta), V(0,r,\theta)] = \sum_{m=-\infty}^{\infty}\sum_{\mu=1}^{\infty}[P_{m\mu}, V_{m\mu}]U_{m\mu}(r)\,\mathrm{e}^{-\mathrm{i}m\theta},$$

where

$$[P_{m\mu}, V_{m\mu}] = \frac{1}{2\pi}\int_0^{2\pi}\int_0^1 [P(0,r,\theta), V(0,r,\theta)]U_{m\mu}(r)\,\mathrm{e}^{\mathrm{i}m\theta}\,r\,\mathrm{d}r\mathrm{d}\theta,$$

The corresponding amplitudes $A_{m\mu}$ and $B_{m\mu}$ are found from identifying

$$P_{m\mu} = A_{m\mu} + B_{m\mu}, \qquad V_{m\mu} = \frac{\sigma^{+}_{m\mu}-M}{1-M\sigma^{+}_{m\mu}}A_{m\mu} + \frac{\sigma^{-}_{m\mu}-M}{1-M\sigma^{-}_{m\mu}}B_{m\mu},$$

leading to (note that $\sigma^{+}_{m\mu} = -\sigma^{-}_{m\mu}$)

$$\begin{aligned} A_{m\mu} &= (1-M\sigma^{+}_{m\mu})\frac{(\sigma^{+}_{m\mu}+M)P_{m\mu} + (1+M\sigma^{+}_{m\mu})V_{m\mu}}{2(1-M^2)\sigma^{+}_{m\mu}}, \\ B_{m\mu} &= (1-M\sigma^{-}_{m\mu})\frac{(\sigma^{-}_{m\mu}+M)P_{m\mu} + (1+M\sigma^{-}_{m\mu})V_{m\mu}}{2(1-M^2)\sigma^{-}_{m\mu}}. \end{aligned} \tag{93}$$

From the axial intensity in hard-walled flow duct (146b)

$$\langle \boldsymbol{I}\cdot\boldsymbol{e}_x\rangle = \tfrac{1}{2}\,\mathrm{Re}\big[(p+Mu)(\overline{u+Mp})\big] \tag{94}$$

we obtain the axial power (148)

$$\mathcal{P} = \pi\beta^4 \sum_{m=-\infty}^{\infty} \sum_{\mu=1}^{\mu_0} \Big[\frac{\sigma^+_{m\mu}|A_{m\mu}|^2}{(1-M\sigma^+_{m\mu})^2} + \frac{\sigma^-_{m\mu}|B_{m\mu}|^2}{(1-M\sigma^-_{m\mu})^2} \Big] \tag{95}$$
$$+ 2\pi\beta^4 \sum_{m=-\infty}^{\infty} \sum_{\mu=\mu_0+1}^{\infty} \frac{\tau_{m\mu}}{(1+M^2\tau^2_{m\mu})^2} \Big[(1-M^2\tau^2_{m\mu}) \operatorname{Im}(A_{m\mu}\overline{B_{m\mu}}) - 2M\tau_{m\mu} \operatorname{Re}(A_{m\mu}\overline{B_{m\mu}}) \Big].$$

$\mu_0 = \mu_0(m)$ is the number of cut-on modes per m, and $\tau_{m\mu} = \mathrm{i}\sigma^+_{m\mu} = -\mathrm{i}\sigma^-_{m\mu}$ is positive real for cut-off modes. Note the coupling between left- and right-running cut-off modes.

5.2 Soft Wall and Uniform Mean Flow

Consider a cylindrical duct with soft wall of specific impedance Z and uniform mean flow of Mach number M. For this configuration the acoustic field allows again modes, similar to the no-flow situation, although their behaviour with respect to possible surface waves is more complicated (Rienstra, 2003; Brambley and Peake, 2006; Vilenski and Rienstra, 2007).

We start with modes of the same form as for the hard wall case (equations 82 with 90, and 91) for pressure p and radial velocity v (we drop the exponential $\mathrm{e}^{\mathrm{i}\omega t - \mathrm{i}m\theta}$)

$$p = \mathrm{e}^{-\mathrm{i}\Omega\sigma X + \mathrm{i}\Omega M X} J_m(\Omega\gamma r), \quad v = \frac{\mathrm{i}\beta\gamma}{1-M\sigma} \mathrm{e}^{-\mathrm{i}\Omega\sigma X + \mathrm{i}\Omega M X} J'_m(\Omega\gamma r),$$

where $\sigma = \pm\zeta(\gamma)$ and the sign of σ is (in general) connected to the direction of propagation[7].

It should be noted that, in contrast to the previous hard-wall with flow, and no flow cases, the radial wavenumber $\alpha = \Omega\gamma$ is *not* left-right symmetric anymore, but depends on the propagation direction. (The boundary condition contains now k, c.q. σ.) So together with $k^\pm_{m\mu}$ and $\sigma^\pm_{m\mu}$ we have to write also $\alpha^\pm_{m\mu}$, $\gamma^\pm_{m\mu}$ and $N^\pm_{m\mu}$.

From the boundary condition (44)we have in dimensionless form

$$\mathrm{i}\omega Z v = \Big(\mathrm{i}\omega + M\frac{\partial}{\partial x}\Big) p$$

we find the equation for reduced axial wave number σ for any given Z, m, and ω

$$(1-M\sigma)^2 J_m(\Omega\gamma) - \mathrm{i}\beta^3 Z\gamma J'_m(\Omega\gamma) = 0. \tag{96}$$

A graphical description of their behaviour as a function of $\operatorname{Im} Z$ (from $+\infty$ down to $-\infty$) and fixed $\operatorname{Re} Z$ is given in the series of figures (17). For large enough frequency, ω, the behaviour of the modes can be classified as follows. When σ is near a hard-wall value, the mode described is really of acoustic nature, extending radially through the whole duct. However, when σ is far enough away from a hard-wall value, the imaginary part of $\Omega\gamma$ becomes significant. The complex Bessel function $J_m(\Omega\gamma r)$ becomes exponentially decaying away from the wall, and the mode is radially restricted to the duct wall region.

[7]Note that if $\sigma = 1/M$, i.e. if $\gamma = \pm\mathrm{i}\beta/M$, we have to rescale the modal amplitude such that $p = 0$. In this case the mode is a pressureless vorticity mode, comparable with footnote 2.

In other words, it has become a surface wave of two-dimensional nature, and approximately[8] described by

$$(1 - M\sigma)^2 + \beta^3 Z\gamma(\sigma) = 0. \tag{97}$$

The "egg" (figure 16), indicating the location of possible surface waves for $\mathrm{Re}(Z) = 0$ in the 2D limit, is drawn in the figures 17 by a dotted line. The 2D surface wave solutions (figure 16) are indicated by black lines. The behaviour of the modes is to a certain extent similar to the no-flow situation (section 4.3, figures 10), although the effect of the mean flow is that we have now 4 rather than 2 possible surface waves. For large $\mathrm{Re}\, Z$, the modes remain near their hard-wall values. For lower values of $\mathrm{Re}\, Z$ the behaviour becomes more irregular. The modes change position with a neighbour, and some become temporarily a surface wave. The two hydrodynamic modes disappear to infinity for $\mathrm{Im}\, Z \to -\infty$.

An example of a modal shape function with impedance walls is given in figure 15.

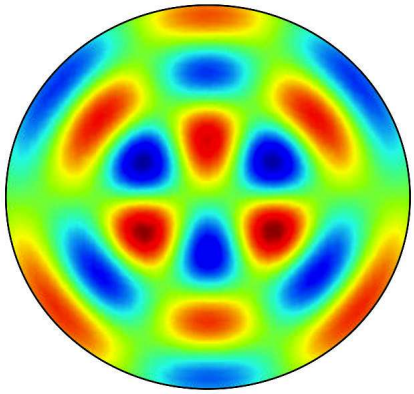

Figure 15: Mode shape for $m = 3$, $\mu = 3$, $\omega = 20$, $Z = 2 + \mathrm{i}$, $M = 0.3$.

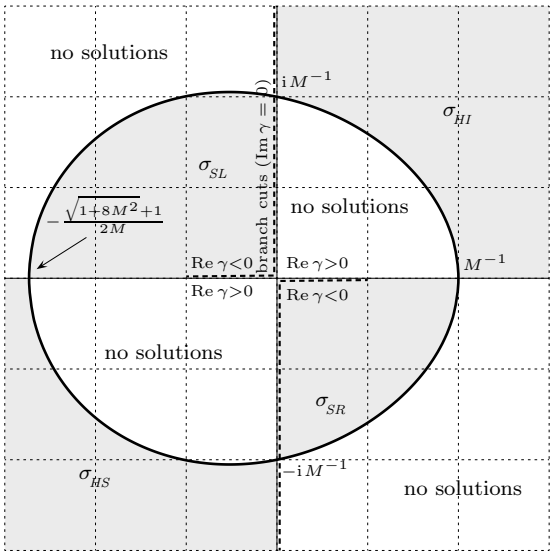

Figure 16: Reduced wave number σ-plane as described by eq. (97), with regions of existence of surface waves. Thick lines map to imaginary Z-axis. Here, $M = 0.5$ is taken.

[8]Note that $J'_m(z)/J_m(z) \sim -\mathrm{i}\,\mathrm{sign}(\mathrm{Im}(z))$ for $|z| \to \infty$, while $\mathrm{Im}(\gamma) < 0$.

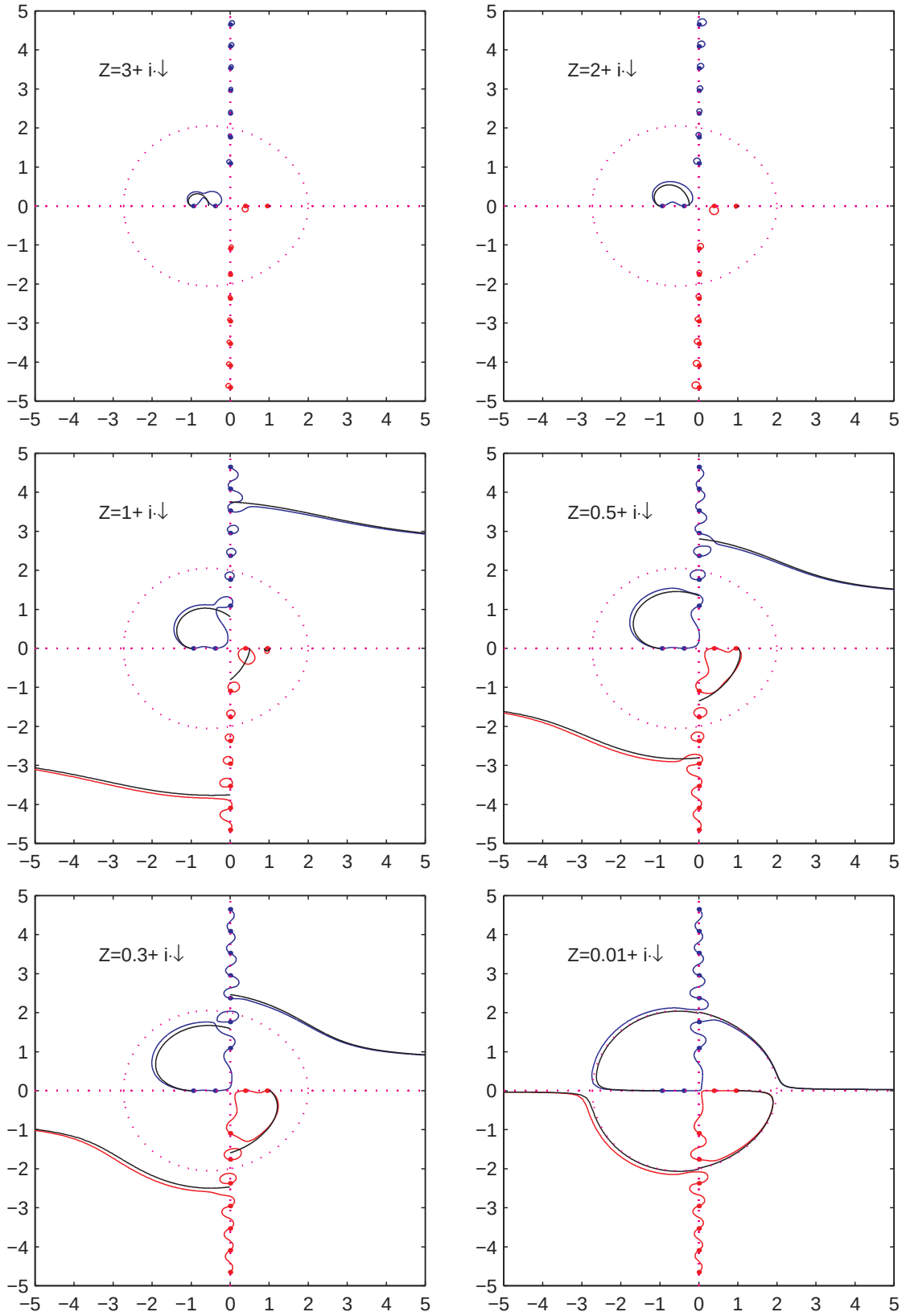

Figure 17: Trajectories of reduced wave number $\sigma_{m\mu}$ ($m = 1$, $\omega = 5$) where $M = 0.5$, for $\mathrm{Im}(Z)$ varying from $-\infty$ to ∞ and fixed $\mathrm{Re}(Z)$. The 2D surface wave solutions of eqn. (97) are included as black lines.

6 Source Expansion

6.1 Modal Amplitudes

A source at $x = 0$, defined by

$$p(0, r, \vartheta) = p_0(r, \vartheta)$$

produces in a hard walled duct a sound field (57a) with modal amplitudes given by

$$A_{m\mu} = \frac{1}{2\pi} \int_0^{2\pi} \int_0^1 p_0(r, \vartheta) U_{m\mu}(r)\, \mathrm{e}^{\mathrm{i}m\vartheta}\, r\, \mathrm{d}r\mathrm{d}\vartheta, \qquad B_{m\mu} = 0 \tag{98}$$

if $x > 0$, and the same in $x < 0$ but with A and B interchanged; apply (63), Note that small details of the source (averaged out for the lower modes in the process of integration), only contribute to higher order modes and do not generate sound if these modes are cut-off.

6.2 Rotating Fan

Of practical interest, especially in aircraft noise reduction (Tyler and Sofrin, 1962), is the following model of a propeller or fan with B identical blades, equally spaced $\Delta\vartheta = 2\pi/B$ radians apart, rotating with angular speed Ω. If at some time $t = 0$ at a fixed position x the field due to one blade is given by the shape function $q(\vartheta, r)$, then from periodicity the total field is described by the sum

$$p(r, \vartheta, 0) = q(\vartheta, r) + q(\vartheta - \Delta\vartheta, r) + \cdots = \sum_{k=0}^{B-1} q\big(\vartheta - \tfrac{2\pi k}{B}, r\big). \tag{99}$$

This function, periodic in ϑ with period $2\pi/B$, may be expanded in a Fourier series:

$$p(\vartheta, r, 0) = \sum_{n=-\infty}^{\infty} q_n(r)\, \mathrm{e}^{-\mathrm{i}nB\vartheta}\,. \tag{100}$$

Since the field is associated to the rotor, it is a function of $\vartheta - \Omega t$. So at a time t

$$p(\vartheta, r, t) = \sum_{k=0}^{B-1} q\big(\vartheta - \Omega t - \tfrac{2\pi k}{B}, r\big) = \sum_{n=-\infty}^{\infty} q_n(r)\, \mathrm{e}^{\mathrm{i}nB\Omega t - \mathrm{i}nB\vartheta} \tag{101}$$

(with $q_{-n} = \overline{q_n}$ because p is real). Evidently, the field is built up from harmonics of the blade passing frequency $B\Omega$. Note that each frequency $\omega = nB\Omega$ is now linked to a circumferential periodicity $m = nB$, and we jump with steps B through the modal m-spectrum. Since the plane wave ($m = 0$) is generated with frequency $\omega = 0$ it is acoustically not interesting, and we may ignore this component. An interesting consequence for a rotor in a duct is the observation that it is not obvious if there is (propagating) sound generated at all: the frequency must be higher than the cut-off frequency. For any harmonic ($n > 0$) we have:

$$f_m = \frac{m\Omega}{2\pi} > \frac{j'_{m1} c_0}{2\pi a} \tag{102}$$

which is for the tip Mach number M_{tip} the condition

$$M_{tip} = \frac{a\Omega}{c_0} > \frac{j'_{m1}}{m}. \tag{103}$$

Since the first zero of J'_m is always (slightly) larger than m (Appendix A.1), it implies that the tip must rotate *supersonically* ($M_{tip} > 1$) for the fan to produce sound.

Of course, in practice a ducted fan with subsonically rotating blades will not be entirely silent. For example, ingested turbulence and the turbulent wake of the blades are not periodic and will therefore not follow this cut-off reduction mechanism. On the other hand, if the perturbations resulting from blade thickness and lift forces alone are dominating as in aircraft engines, the present result is significant, and indeed the inlet fan noise level of many aircraft turbo fan engines is greatly enhanced at take off by the inlet fan rotating supersonically (together with other effects leading to the so-called *buzzsaw noise* (Smith, 1989)).

6.3 Tyler and Sofrin Rule for Rotor-Stator Interaction

The most important noise source of an aircraft turbo fan engine at inlet side is the noise due to interaction between inlet rotor and neighbouring stator.

Behind the inlet rotor, or fan, a stator is positioned (figure 18) to compensate for the rotation, or swirl, in the flow due to the rotor. The viscous and inviscid wakes from the rotor blades hit the stator vanes which results into the generation of sound (Schulten, 1993). A very simple but at the same time very important and widely used device to reduce this sound is the "Tyler and Sofrin selection rule" (Smith, 1989; Tyler and Sofrin, 1962). It is based on elegant manipulation of Fourier series, and amounts to nothing more than a clever choice of the rotor blade and stator vane numbers, to link the first (few) harmonics of the sound to duct modes that are cut-off and therefore do not propagate.

Consider the same rotor as above, with B identical blades, equally spaced $\Delta\vartheta = 2\pi/B$ radians apart, rotating with angular speed Ω, and a stator with V identical vanes, equally spaced $\Delta\vartheta = 2\pi/V$ radians apart. First, we observe that the field generated by rotor-stator interaction must have the time dependence of the rotor, and is therefore built up from harmonics of the blade passing frequency $B\Omega$. Furthermore, it is periodic in ϑ, so it may be written as

$$p(r,\vartheta,t) = \sum_{n=-\infty}^{\infty} Q_n(r,\vartheta)\,\mathrm{e}^{\mathrm{i}nB\Omega t} = \sum_{n=-\infty}^{\infty}\sum_{m=-\infty}^{\infty} Q_{nm}(r)\,\mathrm{e}^{\mathrm{i}nB\Omega t - \mathrm{i}m\vartheta}\,. \tag{104}$$

However, we can do better than that, because most of the m-components are just zero. The field is periodic in ϑ with the stator periodicity $2\pi/V$ in such a way that when we travel with the rotor over an angle $\Delta\vartheta = 2\pi/V$ in a time step $\Delta t = \Delta\vartheta/\Omega$ the field must be the same:

$$p(r,\vartheta,t) = \sum_{n=-\infty}^{\infty}\sum_{m=-\infty}^{\infty} Q_{nm}(r)\,\mathrm{e}^{\mathrm{i}nB\Omega(t-\Delta t) - \mathrm{i}m(\vartheta-\Delta\vartheta)}\,. \tag{105}$$

This yields for any m the restriction: $-\mathrm{i}nB\Omega\Delta t + \mathrm{i}m\Delta\vartheta = 2\pi\mathrm{i}k$, or

$$m = kV + nB \tag{106}$$

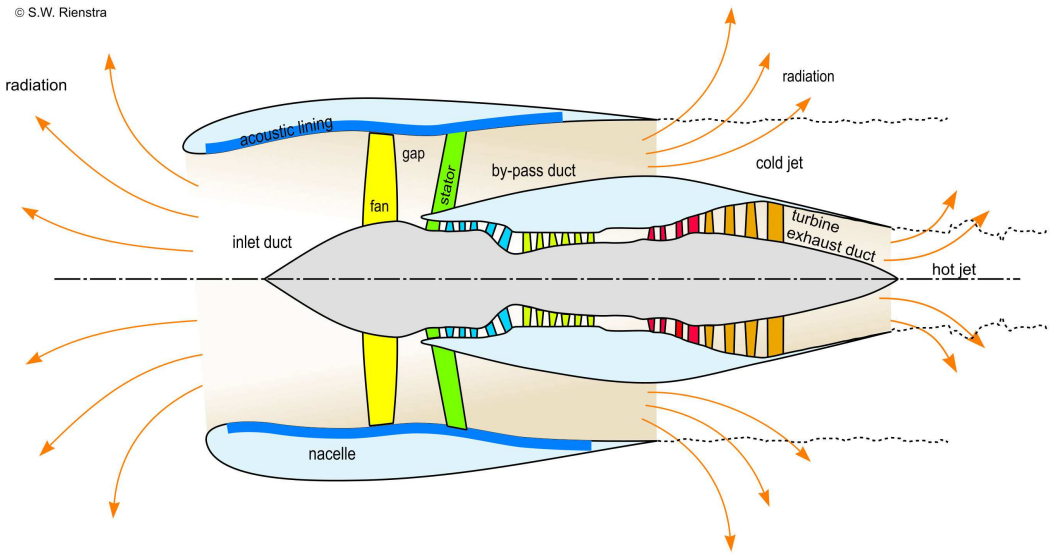

Figure 18: Sketch of high by-pass turbo fan engine. Note the fan (or inlet rotor), which produces with the stator (or outlet guide vanes) the important *rotor-stator interaction* noise. This is to be attenuated by the acoustically lined walls of the inlet and bypass duct.

where k is any integer, and n the harmonic of interest. By selecting B and V such that the lowest $|m|$ possible is high enough for the harmonic of interest to be cut-off, this component is effectively absent for a long enough inlet duct. In practice, only the first harmonic is reduced in this way. A recent development is that the second harmonic, which is usually cut-on, is reduced by selecting the mode number m to be of opposite sign of n, which means: counter rotating with respect to the rotor. In this case the rotor itself acts as a shield obstructing the spiralling modes to leave the duct (Schulten, 1993).

In detail: for a cut-off n-th harmonic (we only have to consider positive n) we need

$$\frac{nB\Omega}{2\pi} < \frac{j'_{m1}c_0}{2\pi a} \quad \text{or} \quad nBM_{tip} < j'_{m1}. \tag{107}$$

Since typically M_{tip} is slightly smaller than 1 and j'_{m1} is slightly larger than $|m|$ we get the evanescent wave condition (all modes are cut off)

$$nB \leqslant |m| = |kV + nB|. \tag{108}$$

The only values of kV for which this inequality is not satisfied automatically is in the interval $-2nB < kV < 0$. If we make the step size V big enough so that we avoid this interval for $k = -1$, we avoid it for any k. So we have finally the condition: $V \geqslant 2nB$.

Consider, as a realistic example, the following configuration of a rotor with $B = 22$ blades and a stator with $V = 55$ vanes. The generated m-modes are for the first two harmonics:

$$\begin{aligned} \text{for } n = 1: &\quad m = \cdots, -33, 22, 77, \cdots \\ \text{for } n = 2: &\quad m = \cdots, -11, 44, 99, \cdots \end{aligned}$$

which indeed corresponds to only cut-off modes of the first harmonic ($m = 22$ and larger) and a counter rotating cut-on second harmonic ($m = -11$).

However elegant, the Tyler-Sofrin rule is no panacea. It is based on the idealisation of a perfectly radially symmetric mean flow. In reality an engine inlet is not symmetric, sometimes "drooped", and (for example due to the presence of the wing) the mean flow is not exactly symmetric and parallel with the duct axis. All these "inlet flow distortions" give rise of so-called distortion modes, not satisfying the Tyler-Sofrin rule.

6.4 Point Source in a Lined Flow Duct

Modes can be considered as building block solutions to express any acoustic field in a duct. They do appear naturally, however, as the poles of the x-Fourier transformed solution of the acoustic problem with a localised source, such that by standard residue calculus these poles produce the solution as a sum over the modes. An example is given below (Rienstra and Tester, 2008).

Consider a cylindrical duct of non-dimensional radius 1, a mean flow of subsonic Mach number M, and harmonic pressure and velocity perturbations p of non-dimensional angular frequency ω. The pressure is excited by a point source at $\boldsymbol{x}_0$, and satisfies the equation

$$\nabla^2 p - \Big(\mathrm{i}\omega + M\frac{\partial}{\partial x}\Big)^2 p = \delta(\boldsymbol{x}-\boldsymbol{x}_0), \tag{109}$$

so $p(\boldsymbol{x};\boldsymbol{x}_0)$ represents the Green's function of the system. Note the $\mathrm{e}^{\mathrm{i}\omega t}$ - convention. The impedance boundary condition at $r=1$ (44), becomes in terms of the pressure

$$\Big(\mathrm{i}\omega + M\frac{\partial}{\partial x}\Big)^2 p + \mathrm{i}\omega Z\frac{\partial p}{\partial r} = 0 \quad \text{at} \quad r=1. \tag{110}$$

For a hollow duct finiteness of p is assumed at $r=0$. Finally, we adopt radiation conditions that says that we only accept solutions that radiate away from the source position $\boldsymbol{x}_0$.

We represent the delta-function by a generalised Fourier series in ϑ and Fourier integral in x

$$\delta(\boldsymbol{x}-\boldsymbol{x}_0) = \frac{\delta(r-r_0)}{r_0}\frac{1}{2\pi}\int_{-\infty}^{\infty}\mathrm{e}^{-\mathrm{i}\kappa(x-x_0)}\,\mathrm{d}\kappa\,\frac{1}{2\pi}\sum_{m=-\infty}^{\infty}\mathrm{e}^{-\mathrm{i}m(\vartheta-\vartheta_0)}. \tag{111}$$

where $0<r_0<1$, and write accordingly

$$p(x,r,\vartheta) = \sum_{m=-\infty}^{\infty}\mathrm{e}^{-\mathrm{i}m(\vartheta-\vartheta_0)}\,p_m(r,x) = \sum_{m=-\infty}^{\infty}\mathrm{e}^{-\mathrm{i}m(\vartheta-\vartheta_0)}\int_{-\infty}^{\infty}\hat{p}_m(r,\kappa)\,\mathrm{e}^{-\mathrm{i}\kappa(x-x_0)}\,\mathrm{d}\kappa. \tag{112}$$

Substitution of (111) and (112) in (109) yields for $\hat{p}_m$

$$\frac{\partial^2\hat{p}_m}{\partial r^2} + \frac{1}{r}\frac{\partial\hat{p}_m}{\partial r} + \Big(\alpha^2 - \frac{m^2}{r^2}\Big)\hat{p}_m = \frac{\delta(r-r_0)}{4\pi^2 r_0}, \tag{113}$$

with

$$\alpha^2 = \Omega^2 - \kappa^2, \quad \Omega = \omega - \kappa M. \tag{114}$$

This has solution

$$\hat{p}_m(r,\kappa) = A(\kappa)J_m(\alpha r) + \frac{1}{8\pi}H(r-r_0)\big(J_m(\alpha r_0)Y_m(\alpha r) - Y_m(\alpha r_0)J_m(\alpha r)\big) \tag{115}$$

where H denotes Heaviside stepfunction, and use is made of the Wronskian (132). $A(\kappa)$ is to be determined from the boundary conditions at $r = 1$, which is (assuming uniform convergence of the $m-$modal series) per mode

$$\mathrm{i}\Omega^2 \hat{p}_m + \omega Z \hat{p}'_m = 0 \quad \text{at} \quad r = 1. \tag{116}$$

(The prime denotes a derivative to r). This yields

$$A = \frac{1}{8\pi}\left[Y_m(\alpha r_0) - \frac{\mathrm{i}\Omega^2 Y_m(\alpha) + \omega\alpha Z Y'_m(\alpha)}{\mathrm{i}\Omega^2 J_m(\alpha) + \omega\alpha Z J'_m(\alpha)} J_m(\alpha r_0)\right],$$

and thus

$$\hat{p}_m(r,\kappa) = J_m(\alpha r_<)\frac{\mathrm{i}\Omega^2 G_m(r_>,\alpha) + \omega Z H_m(r_>,\alpha)}{8\pi E_m(\kappa)},$$

where $r_> = \max(r, r_0)$, $r_< = \min(r, r_0)$ and

$$\begin{aligned} E_m(\kappa) &= \mathrm{i}\Omega^2 J_m(\alpha) + \omega\alpha Z J'_m(\alpha) \\ G_m(r,\alpha) &= J_m(\alpha)Y_m(\alpha r) - Y_m(\alpha)J_m(\alpha r) \\ H_m(r,\alpha) &= \alpha J'_m(\alpha)Y_m(\alpha r) - \alpha Y'_m(\alpha)J_m(\alpha r) \end{aligned}$$

By substituting the defining series we find that G_m and H_m are analytic functions of α^2, while both E_m and $J_m(\alpha r_<)$ can be written as α^m times an analytic function of α^2. As a result, $\hat{p}_m(r,\kappa)$ is a meromorphic[9] function of κ. It has isolated poles $\kappa = k^{\pm}_{m\mu}$, given by

$$E_m(k^{\pm}_{m\mu}) = 0,$$

which is equivalent to (96). The final solution is found by Fourier back-transformation: close the integration contour around the lower half plane for $x > x_0$ to enclose the complex modal wave numbers of the right-running modes, and the upper half plane for $x < x_0$ to enclose the complex modal wave numbers of the left-running modes. In figure 19 a typical location of the integration contour with no-flow modes is shown. See also figures 10, 11 and 17.

We define

$$Q_{m\mu} = \pm\left[(k^{\pm}_{m\mu} + \Omega^{\pm}_{m\mu}M)\Big(1 - \frac{m^2}{(\alpha^{\pm}_{m\mu})^2} - \frac{(\Omega^{\pm}_{m\mu})^4}{(\omega\alpha^{\pm}_{m\mu}Z)^2}\Big) - \frac{2\mathrm{i}M\Omega^{\pm}_{m\mu}}{\omega Z}\right],$$

where $+/-$ relates to right/left-running modes. With the result

$$\left.\frac{\mathrm{d}E_m}{\mathrm{d}\kappa}\right|_{\kappa=k^{\pm}_{m\mu}} = \pm\omega Z Q_{m\mu} J_m(\alpha^{\pm}_{m\mu})$$

the integral is evaluated as a sum over the residues in the poles at $\kappa = k^{+}_{m\mu}$ for $x > x_0$ and at $k^{-}_{m\mu}$ for $x < x_0$. From eigenvalue equation $E_m(k^{\pm}_{m\mu}) = 0$ and the Wronskian (132) we obtain

$$\mathrm{i}\Omega^2_{m\mu} G_m(r_>,\alpha_{m\mu}) + \omega Z H_m(r_>,\alpha_{m\mu}) = -\frac{2\omega Z}{\pi J_m(\alpha_{m\mu})} J_m(\alpha_{m\mu} r_>).$$

[9] A *meromorphic* function is analytic on the complex plane except for isolated poles.

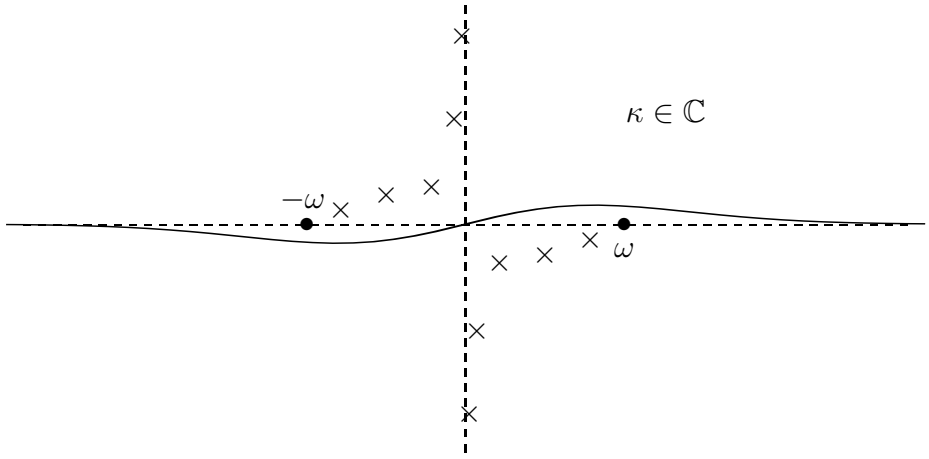

Figure 19: Contour of integration in the κ-plane.

where $\alpha_{m\mu} = \alpha(k_{m\mu})$. We can skip the distinction between $r_>$ and $r_<$ and achieve the soft wall modal expansion

$$p_m(r,x) = -\frac{1}{2\pi \mathrm{i}} \sum_{\mu=1}^{\infty} \frac{J_m(\alpha_{m\mu} r) J_m(\alpha_{m\mu} r_0)}{Q_{m\mu} J_m^2(\alpha_{m\mu})} \, \mathrm{e}^{-\mathrm{i} k_{m\mu}(x-x_0)} \tag{117}$$

where for $x > x_0$ the sum pertains to the right-running waves, corresponding to the modal wave numbers $k^+_{m\mu}$ found in the lower complex half plane, and for $x < x_0$ the left-running waves, corresponding to $k^-_{m\mu}$ found in the upper complex half plane (Rienstra and Tester, 2008).

Only if a mode from the upper half plane is to be interpreted as a right-running instability (the necessary analysis is subtle, and involves the $\omega-$dependence of Z (Brambley et al., 2012; Rienstra and Darau, 2011)), its contribution is to be excluded from the set of modes for $x < x_0$ and included in the modes for $x > x_0$. The form of the solution remains exactly the same, as we do no more than deforming the integration contour into the upper half plane.

It may be noted that expression (117) is continuous in (x, r), except at (x_0, r_0) where the series slowly diverges like a harmonic series. As may be expected from the symmetry of the configuration, the clockwise and anti-clockwise rotating circumferential modes are equal, i.e. $p_m(r,x) = p_{-m}(r,x)$.

Solution (117) is very general. It includes both the no-flow solution (take $M = 0$) and the hard walled duct (take $Z = \infty$). Without mean flow the problem becomes symmetric in x and it may be notationally convenient to write $\alpha^{\pm}_{m\mu} = \alpha_{m\mu}$, $k^+_{m\mu} = k_{m\mu}$ and $k^-_{m\mu} = -k_{m\mu}$.

Finding all the eigenvalues $k^{\pm}_{m\mu}$ is evidently crucial for the evaluation of the series (117), in particular when surface waves (compare with figures 17 and 16) occur. Examples of $p_m(x,r)$ are plotted in figures 20 and 21.

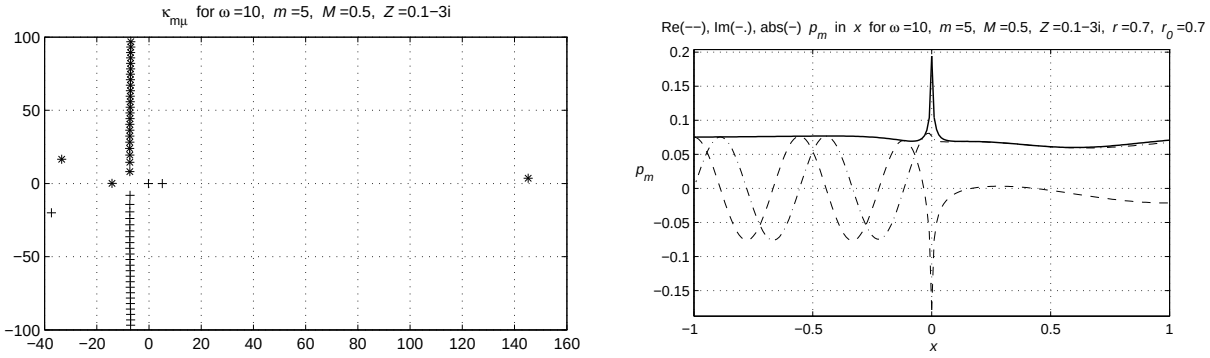

Figure 20: Eigenvalues $k^{\pm}_{m\mu}$ and $\mathrm{Re}(p_m)$, $\mathrm{Im}(p_m)$ and $|p_m|$ is plotted of the $m = 5$-th component of the point source field in a lined flow duct with $\omega = 10$, $Z = 0.1 - 3\mathrm{i}$, $x_0 = 0$, $r_0 = 0.7$, $M = 0.5$ at $r = 0.7$ and $\theta = \theta_0$. Note the presence of 3 surface waves.

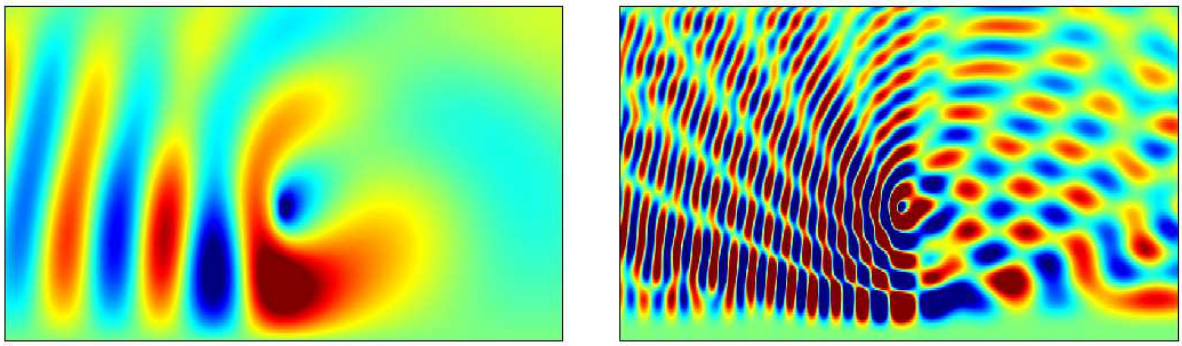

Figure 21: Snapshots of p_m field for $\omega = 10$, $m = 1$, $Z = 2 + \mathrm{i}$ (left), and $\omega = 50$, $m = 5$, $Z = 2 - \mathrm{i}$ (right) and $M = 0.5$ and $r_0 = 0.4$ in both cases

6.5 Point Source in a Duct Wall

A problem, closely related to the previous one, is the field from a source $\boldsymbol{v}\cdot\boldsymbol{e}_r = -\delta(\boldsymbol{x}-\boldsymbol{x}_0)$ in the duct wall $r = 1$. Consider for simplicity a hard-walled duct without mean flow. We have for the pressure

$$\frac{1}{\mathrm{i}\omega}\frac{\partial p}{\partial r}\bigg|_{r=1} = \frac{1}{2\pi}\int_{-\infty}^{\infty} \mathrm{e}^{-\mathrm{i}\kappa(x-x_0)}\,\mathrm{d}\kappa\,\frac{1}{2\pi}\sum_{m=-\infty}^{\infty}\mathrm{e}^{-\mathrm{i}m(\vartheta-\vartheta_0)}\,. \tag{118}$$

We solve equation (4) again via Fourier transformation in x, and Fourier series expansion in ϑ. We obtain

$$p(x,r,\vartheta) = \sum_{m=-\infty}^{\infty}\mathrm{e}^{-\mathrm{i}m(\vartheta-\vartheta_0)}\int_{-\infty}^{\infty} A_m(\kappa)J_m(\alpha(\kappa)r)\,\mathrm{e}^{-\mathrm{i}\kappa(x-x_0)}\,\mathrm{d}\kappa \tag{119}$$

where $\alpha(\kappa)^2 = \omega^2 - \kappa^2$. From the Fourier transformed boundary condition (118) it follows that $\alpha A_m J_n'(\alpha) = -\omega/4\pi^2\mathrm{i}$, so

$$p(x,r,\vartheta) = -\frac{\omega}{4\pi^2\mathrm{i}}\sum_{m=-\infty}^{\infty}\mathrm{e}^{-\mathrm{i}m(\vartheta-\vartheta_0)}\int_{-\infty}^{\infty}\frac{J_m(\alpha r)}{\alpha J_m'(\alpha)}\,\mathrm{e}^{-\mathrm{i}\kappa(x-x_0)}\,\mathrm{d}\kappa.$$

The poles of the meromorphic integrand are found at $\kappa = \pm k_{m\mu}$ (we use the symmetry in x), and since the waves must be outgoing the integration contour in the κ-plane must be located as in figure 19. Closing the contour via $\mathrm{Im}(\kappa) \to -\infty$ for $x > 0$ and via $\mathrm{Im}(\kappa) \to +\infty$ yields the solution, in the form of a series over the residue-contributions[10] in $\kappa = \pm k_{m\mu}$. This yields the modal expansion

$$p(x, r, \vartheta) = \frac{\omega}{2\pi} \sum_{m=-\infty}^{\infty} \sum_{\mu=1}^{\infty} \frac{J_m(\alpha_{m\mu} r)\, \mathrm{e}^{-\mathrm{i}k_{m\mu}|x-x_0| - \mathrm{i}m(\vartheta-\vartheta_0)}}{(1 - m^2/\alpha_{m\mu}^2) J_m(\alpha_{m\mu}) k_{m\mu}}. \tag{120}$$

The contribution of the $m = 0, \mu = 1$ plane-wave mode is

$$\frac{1}{2\pi}\, \mathrm{e}^{-\mathrm{i}\omega|x|}\,.$$

[10] Near $\kappa = k_{m\mu}$ is $J'_m(\alpha(\kappa)) \simeq -(\kappa - k_{m\mu}) k_{m\mu} \alpha_{m\mu}^{-1} J''_m(\alpha_{m\mu})$.

7 Reflection and Transmission

7.1 A Discontinuity in Diameter

One single modal representation is only possible in segments of a duct with constant properties (diameter, wall impedance). When two segments of different properties are connected to each other we can use a modal representation in each segment, but since the modes are different we have to reformulate the expansion of the incident field into an expansion of the transmitted field in the neighbouring segment, using conditions of continuity of pressure and velocity. This is called: *mode matching*. Furthermore, these continuity conditions cannot be satisfied with a transmission field only, and a part of the incident field is reflected. Each mode is scattered into a modal spectrum of transmitted and reflected modes.

Consider a duct with a discontinuity in diameter at $x = 0$ (figure 22): a radius a along $x < 0$ and a radius b along $x > 0$, with (for definiteness) $a > b$. Because of circumferential symmetry there is no scattering into other m-modes, so we will consider only a single m-mode. The field p_{in}, incident from $x = -\infty$ and given by (see equation 56)

$$p_{in} = \sum_{\mu=1}^{\infty} A_{m\mu} U_{m\mu}(r)\, \mathrm{e}^{-\mathrm{i}k_{m\mu}x - \mathrm{i}m\vartheta}, \tag{121a}$$

is scattered at $x = 0$ into the reflected wave p_{ref}

$$p_{ref} = \sum_{\mu=1}^{\infty} B_{m\mu} U_{m\mu}(r)\, \mathrm{e}^{\mathrm{i}k_{m\mu}x - \mathrm{i}m\vartheta}, \tag{121b}$$

$$B_{m\mu} = \sum_{\nu=1}^{\infty} R_{m\mu\nu} A_{m\nu}, \quad \text{or} \quad \boldsymbol{B} = \mathcal{R}\boldsymbol{A},$$

and into the transmitted wave p_{tr}

$$p_{tr} = \sum_{\mu=1}^{\infty} C_{m\mu} \hat{U}_{m\mu}(r)\, \mathrm{e}^{-\mathrm{i}\ell_{m\mu}x - \mathrm{i}m\vartheta}, \tag{121c}$$

$$\hat{U}_{m\mu}(r) = \hat{N}_{m\mu} J_m(\beta_{m\mu} r),$$

$$C_{m\mu} = \sum_{\nu=1}^{\infty} T_{m\mu\nu} A_{m\nu}, \quad \text{or} \quad \boldsymbol{C} = \mathcal{T}\boldsymbol{A}.$$

$\hat{U}_{m\mu}(r)$ and $\hat{N}_{m\mu}$ are the obvious generalisations of $U_{m\mu}(r)$ and $N_{m\mu}$ on the interval $[0, b]$. Suitable conditions of convergence of the infinite series are assumed, while

$$\alpha_{m\mu} = j'_{m\mu}/a, \quad k_{m\mu} = \sqrt{\omega^2 - \alpha_{m\mu}^2}, \quad \mathrm{Im}(k_{m\mu}) \leqslant 0,$$
$$\beta_{m\mu} = j'_{m\mu}/b\,, \quad \ell_{m\mu} = \sqrt{\omega^2 - \beta_{m\mu}^2}\,, \quad \mathrm{Im}(\ell_{m\mu}) \leqslant 0.$$

The matrices $\mathcal{R}$ and $\mathcal{T}$ are introduced to use the fact that each incident mode reflects and transmits into a modal spectrum. When acting on the incident field amplitude vector $\boldsymbol{A}$, they produce the reflection and transmission field amplitude vectors $\boldsymbol{B}$ and $\boldsymbol{C}$. Therefore, they are called "reflection matrix" and "transmission matrix".

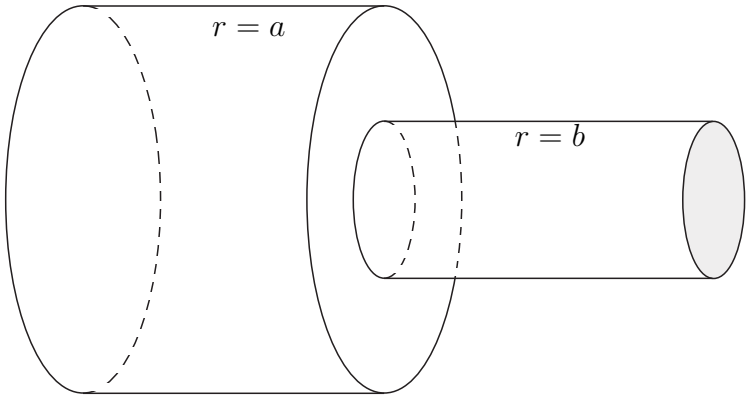

Figure 22: Duct with discontinuous diameter.

At the walls we have the boundary condition of vanishing normal velocity. At the interface $x = 0, 0 \leqslant r \leqslant b$ we have continuity of pressure and axial velocity.

At the edges we have the so-called *edge condition* (Mittra and Lee, 1971): the energy integral of the field in a neighbourhood of an edge must be finite (no source hidden in the edge). This condition is necessary in a geometry with edges because the boundary conditions lose their meaning at an edge, whereas the differential equation is not valid at the boundary. In the context of modal series expansions this condition is related to the convergence rate of the series. A δ-function type of a spurious edge source generates a divergent series expansion (to be interpreted as a generalised function). Although its rôle remains in the usual engineering practice somewhat in the background, the edge condition is certainly important in the present problem.

Since the problem is linear it is sufficient to determine the scattered field of a single μ-mode. It then follows that the continuity of pressure at the interface

$$\sum_{\nu=1}^{\infty}(R_{m\nu\mu} + \delta_{\nu\mu})U_{m\nu} = \sum_{\nu=1}^{\infty} T_{m\nu\mu}\hat{U}_{m\nu} \tag{122}$$

yields, after multiplication with $\hat{U}_{m\lambda}(r)r$, integration from 0 to b, and using orthonormality, the following relation[11] to express $T_{m\lambda\mu}$ in the vector $R_{m\cdot\mu}$:

$$\sum_{\nu=1}^{\infty}\big\langle \hat{U}_{m\lambda}\,, U_{m\nu}\big\rangle_b (R_{m\nu\mu} + \delta_{\nu\mu}) = T_{m\lambda\mu}, \tag{123}$$

where

$$\big\langle f\,, g\big\rangle_b = \int_0^b f(r)g(r)r\,\mathrm{d}r.$$

This integral may be evaluated by using equations (142). The continuity of axial velocity at the interface

$$\sum_{\nu=1}^{\infty} k_{m\nu}(R_{m\nu\mu} - \delta_{\nu\mu})U_{m\nu} = -\sum_{\nu=1}^{\infty} \ell_{m\nu}T_{m\nu\mu}\hat{U}_{m\nu} \tag{124}$$

[11] $\delta_{ij} = 1$ if $i = j$, $\delta_{ij} = 0$ if $i \neq j$.

yields, after multiplication with $U_{m\lambda}(r)r$, integration from 0 to a of the left hand side, and from 0 to b of the right hand side, using $p_x = 0$ on $b \leqslant r \leqslant a$, the following relation expressing $R_{m\lambda\mu}$ in the vector $T_{m\cdot\mu}$:

$$k_{m\lambda}(R_{m\lambda\mu} - \delta_{\lambda\mu}) = -\sum_{\nu=1}^{\infty} \left\langle U_{m\lambda}, \hat{U}_{m\nu} \right\rangle_b \ell_{m\nu} T_{m\nu\mu}. \tag{125}$$

Both equations (123) and (125) are valid for any λ and μ, so we can write in matrix notation

$$\begin{aligned} \mathcal{M}(\mathcal{R} + I) &= \mathcal{T}, \\ \boldsymbol{k}\,(\mathcal{R} - I) &= \mathcal{M}^\top \boldsymbol{\ell}\, \mathcal{T}, \end{aligned} \tag{126}$$

for identity matrix I, matrix $\mathcal{M}$ and its transpose $\mathcal{M}^\top$, and diagonal matrices $\boldsymbol{k}$ and $\boldsymbol{\ell}$, given by

$$\mathcal{M}_{\lambda\nu} = \left\langle \hat{U}_{m\lambda}, U_{m\nu} \right\rangle_b, \quad \boldsymbol{k}_{\lambda\nu} = \delta_{\lambda\nu} k_{m\lambda}, \quad \boldsymbol{\ell}_{\lambda\nu} = \delta_{\lambda\nu} \ell_{m\lambda}.$$

So we have formally the solution

$$\mathcal{R} = (\boldsymbol{k} - \mathcal{M}^\top \boldsymbol{\ell} \mathcal{M})^{-1} (\boldsymbol{k} + \mathcal{M}^\top \boldsymbol{\ell} \mathcal{M}) \tag{127}$$

which can be evaluated by standard techniques for any sufficiently large truncated matrices.

A suitable choice of truncation (Masterman and Clarricoats, 1971; Masterman et al., 1969; Rienstra, 1992; Wu, 1973), allowing for a certain balance between the accuracy in $x < 0$ and in $x > 0$, is to include proportionally more terms in the wider duct: a truncation of the series of (123) after, say, P terms and of (125) after Q terms, with $P/a \simeq Q/b$. This gives truncated matrices $\mathcal{M}_{Q\times P}$, $\mathcal{M}^\top_{P\times Q}$, $\boldsymbol{k}_{P\times P}$, $\boldsymbol{\ell}_{Q\times Q}$, so that we obtain $\mathcal{R}_{P\times P}$ and $\mathcal{T}_{Q\times P}$.

It should be noted that if we take P/Q very much different from a/b, we *may* converge for $P, Q \to \infty$ to another solution (127) than the physical one. This is not an artefact of the method: the solution is indeed not unique, because we have not yet explicitly satisfied the edge condition. The behaviour near the edge depends on the way we let P and Q tend to infinity, and the edge condition is satisfied if their ratio remains: $P/Q \simeq a/b$.

The Iris Problem

When an abrupt contraction of the duct diameter is immediately followed by an expansion to the previous diameter (an infinitely thin orifice plate), we call this an iris. In this case one might be tempted to solve the problem directly by matching the modal expansions at either side of the iris plate. This solution will, however, either not or very slowly converge to the correct (i.e. physical) solution.

The above method of section 7.1, however, is well applicable to this problem too, if we consider the iris as a duct (albeit of zero length) connecting the two main ducts at either side of the iris. Each transition (from duct 1 to the iris, and from the iris to duct 2) is to be treated as above. Since the matrices of each transition are similar, the final system of matrix equations may be further simplified (Rienstra, 1992).

7.2 Open End Reflection

The reflection and diffraction at and radiation from an open pipe end of a modal sound wave depends on the various problem parameters like Helmholtz number ω, mode numbers m, μ and pipe wall thickness. A canonical problem amenable to analysis is that of a hard-walled, cylindrical, semi-infinite pipe of vanishing wall thickness. The exact solution (by means of the Wiener-Hopf technique) was first found by Levine and Schwinger (for $m = 0$) in their celebrated paper (Levine and Schwinger, 1948). Generalisations for higher modes may be found in (Weinstein, 1974) and with uniform (Rienstra, 1984) or jet mean flow (Munt, 1977, 1990).

Inside the pipe we have the incident mode with reflected field, given by $p(x, r, \vartheta) = p_{m\mu}(x, r)\,\mathrm{e}^{-\mathrm{i}m\vartheta}$ where

$$p_{m\mu}(x,r) = U_{m\mu}(r)\,\mathrm{e}^{-\mathrm{i}k_{m\mu}x} + \sum_{\nu=1}^{\infty} R_{m\mu\nu}U_{m\nu}(r)\,\mathrm{e}^{\mathrm{i}k_{m\nu}x}\,. \tag{128}$$

Outside the pipe we have in the far field

$$p_{m\mu}(x,r) \simeq D_{m\mu}(\xi)\frac{\mathrm{e}^{-\mathrm{i}\omega\varrho}}{\omega\varrho} \qquad (\omega\varrho \to \infty), \tag{129}$$

where $x = \varrho\cos\xi$, $r = \varrho\sin\xi$, and $D_{m\mu}(\xi)$ is called the directivity function, and $|D_{m\mu}(\xi)|$ is the radiation pattern.

The reflection matrix $\{R_{m\mu\nu}\}$ and the directivity function are both described by complex integrals, which have to be evaluated numerically. Some important properties are:

- At resonance $\omega = \alpha_{m\mu}$ we have total reflection in itself, $R_{m\mu\mu} = -1$, and no reflection in any other mode, $R_{m\mu\nu} = 0$.
- Near resonance $\omega \sim \alpha_{m\mu}$ the modulus $|R_{m\mu\nu}(\omega)|$ behaves linearly from the left, and like a square root from the right side; the behaviour of the phase $\arg(R_{m\mu\nu}(\omega))$ is similar but reversed: linearly from the right and like a square root from the left.
- A reciprocity relation between the μ, ν and the ν, μ-coefficients:
  $k_{m\nu}R_{m\mu\nu} = k_{m\mu}R_{m\nu\mu}$.
- In the forward arc, $0 < \xi < \frac{1}{2}\pi$, $D_{m\mu}(\xi)$ consists of lobes (maxima interlaced by zeros), while $D_{01}(0) = \frac{1}{2}\sqrt{2}\,\mathrm{i}\omega^2$ and $D_{m\mu}(0) = 0$.
- In the rearward arc, $\frac{1}{2}\pi \leqslant \xi < \pi$, $D_{m\mu}(\xi)$ is free of zeros, and tends to zero for $\xi \to \pi$ if $m \geqslant 1$ and to a finite value if $m = 0$.
- If $k_{m\nu}$ is real and $\nu \neq \mu$, the zeros of $D_{m\mu}(\xi)$ are found at
  $\xi = \arcsin(\alpha_{m\nu}/\omega)$.
- If the mode is cut on, the main lobe is located at
  $\xi_{m\mu} = \arcsin(\alpha_{m\mu}/\omega)$.
- If $\omega \to 0$, the radiation pattern of the plane wave $m\mu = 01$ becomes spherically shaped and small like $O(\omega^2)$, while the reflection coefficient becomes $R_{011} \simeq -\exp(-\mathrm{i}\,2\delta\omega)$, where $\delta = 0.6127$. The dimensional distance δa is called the end correction, since $x = \delta a$ is a fictitious point just outside the pipe, at which the wave appears to reflect with $p = 0$.

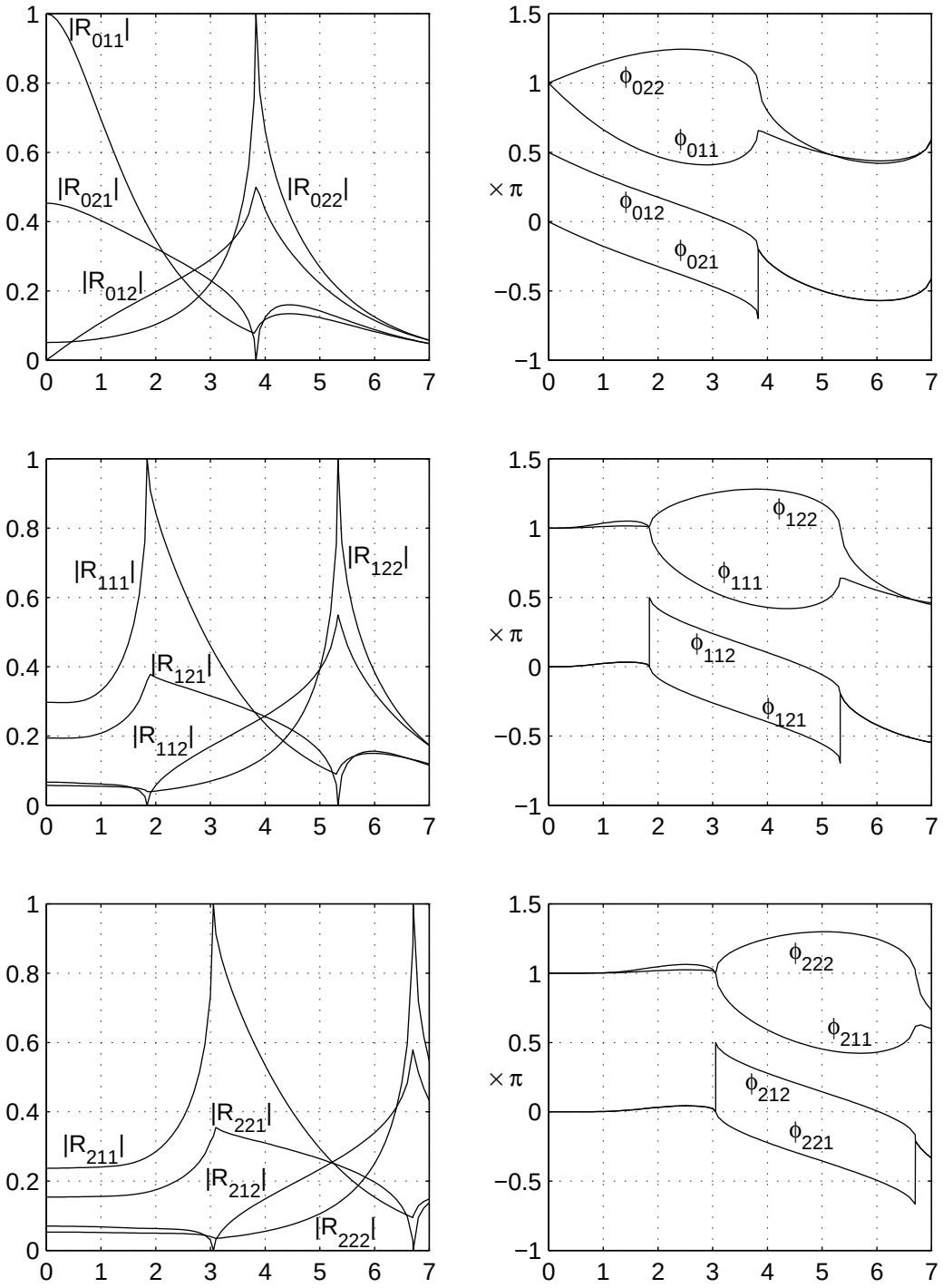

Figure 23: Modulus and phase of reflection coefficients $R_{m\mu\nu}$ for $m = 0 \ldots 2$, $\mu, \nu = 1, 2$, as a function of $\omega = 0 \ldots 7$.

Based on the method presented in (Rienstra, 1984), plots of $R_{m\mu\nu}$ and $|D_{m\mu}(\xi)|$ may be generated, as given in figures 23 and 24.

Of the reflection coefficient we have plotted modulus $|R_{m\mu\nu}(\omega)|$ and phase $\phi_{m\mu\nu} = \arg(R_{m\mu\nu})$ as a function of $\omega = 0 \ldots 7.$, for $m = 0 \ldots 2$ and $\mu, \nu = 1, 2$. Note that the resonance (cut-off) frequencies are $\omega = 3.8317$ and 7.0156 for $m = 0$, $\omega = 1.8412$ and 5.3314 for $m = 1$, and $\omega = 3.0542$ and 6.7061 for $m = 2$.

The radiation pattern is plotted, on dB-scale, of the first radial mode ($\mu = 1$) for $m = 0$ and $m = 1$, and $\omega = 2, 4, 6$. For $m = 0$ the main lobe is at $\xi_{01} = 0$, while the zeros are found for $\omega = 4$ at $\xi = 73.3°$, and for $\omega = 6$ at $\xi = 39.7°$. For $m = 1$ we have the main lobe at $\xi_{11} = 67.0°, 27.4°, 17.9°$ for $\omega = 2, 4, 6$. The zero is found at $\xi = 62.7°$ for $\omega = 6$.

Furthermore, the trend is clear that for higher frequencies the refraction effects become smaller, and the sound radiates more and more like rays (Chapman, 1994). It is instructive to compare the wave front velocity of a mode (the sound speed, dimensionless 1) and the axial phase velocity v_f (66). As the mode spirals through the duct, the wave front makes an angle $\xi_{m\mu}$ with the x-axis such that $\cos(\xi_{m\mu}) = 1/v_f = k_{m\mu}/\omega$. Indeed,

$$\xi_{m\mu} = \arccos(k_{m\mu}/\omega) = \arcsin(\alpha_{m\mu}/\omega)$$

is the angle at which the mode radiates out of the open end, i.e. the angle of the main lobe.

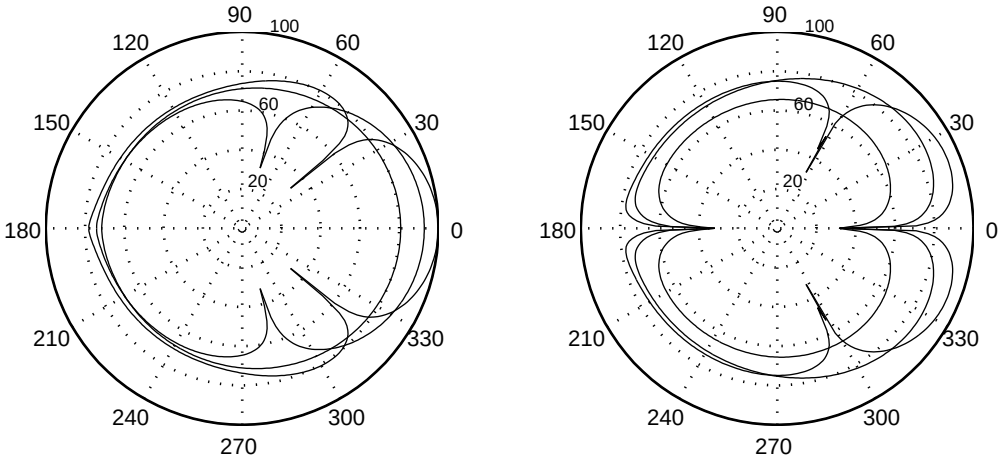

Figure 24: Radiation pattern $20\log_{10}|D_{m\mu}| + 71.7$ for $m\mu = 01, = 11$ and $\omega = 2, 4, 6$.

References

Abramowitz, M. and Stegun, I., editors (1964). *Handbook of Mathematical Functions*, New York. National Bureau of Standards, Dover Publications, Inc.

Brambley, E. (2009). Fundamental problems with the model of uniform flow over acoustic linings. *Journal of Sound and Vibration*, 322:1026–1073.

Brambley, E., Darau, M., and Rienstra, S. (2012). The critical layer in linear-shear boundary layers over acoustic linings. *Journal of Fluid Mechanics*, 710:545–568.

Brambley, E. and Peake, N. (2006). Classification of aeroacoustically relevant surface modes in cylindrical lined ducts. *Wave Motion*, 43:301–310.

Chapman, C. (1994). Sound radiation from a cylindrical duct. Part 1. Ray structure of the duct modes and of the external field. *Journal of Fluid Mechanics*, 281:293–311.

Erdelyi, A., Magnus, W., Oberhettinger, F., and Tricomi, F. (1953). *Higher Transcendental Functions, 3 Volumes*. McGraw-Hill Book Company, Inc., New York.

Goldstein, M. (1976). *Aeroacoustics*. McGraw-Hill Book Company, Inc., New York.

Gradshteyn, I. and Ryzhik, I. (1994). *Table of Integrals, Series and Products*. Academic Press, London, 5th edition. Alan Jeffrey, editor.

Ingard, K. (1959). Influence of fluid motion past a plane boundary on sound reflection, absorption, and transmission. *Journal of the Acoustical Society of America*, 31(7):1035–1036.

Levine, H. and Schwinger, J. (1948). On the radiation of sound from an unflanged circular pipe. *Physical Review*, 73:383–406.

Luke, Y. (1969). *The Special Functions and their Approximations Vol.1 and Vol.2*, volume 53 of *Mathematics in Science and Engineering*. Academic Press, New York, London.

Masterman, P. and Clarricoats, P. (1971). Computer field-matching solution of waveguide transverse discontinuities. *Proc. IEE*, 118(1):51–63.

Masterman, P., Clarricoats, P., and Hannaford, C. (1969). Computer method of solving waveguide-iris problems. *Electronics Letters*, 5(2):23–25.

Mittra, R. and Lee, S. (1971). *Analytical Techniques in the Theory of Guided Waves*. The MacMillan Company, New York.

Morfey, C. (1971). Sound transmission and generation in ducts with flow. *Journal of Sound and Vibration*, 14:37–55.

Munt, R. (1977). The interaction of sound with a subsonic jet issuing from a semi-infinite cylindrical pipe. *Journal of Fluid Mechanics*, 83(4):609–640.

Munt, R. (1990). Acoustic radiation properties of a jet pipe with subsonic jet flow: I. the cold jet reflection coefficient. *Journal of Sound and Vibration*, 142(3):413–436.

Myers, M. (1980). On the acoustic boundary condition in the presence of flow. *Journal of Sound and Vibration*, 71(3):429–434.

Myers, M. (1991). Transport of energy by disturbances in arbitrary flows. *Journal of Fluid Mechanics*, 226:383–400.

Oppeneer, M., Rienstra, S., and Sijtsma, P. (2016). Efficient mode-matching based on closed form integrals of Pridmore-Brown modes. *AIAA Journal*, 54(1):266–279.

Rienstra, S. (1984). Acoustic radiation from a semi-infinite annular duct in a uniform subsonic mean flow. *Journal of Sound and Vibration*, 94(2):267–288.

Rienstra, S. (1992). Acoustical detection of obstructions in a pipe with a temperature gradient. In Van der Burgh, A. and Simonis, J., editors, *Topics in Engineering Mathematics*, pages 151–179. Kluwer Acad. Publishers, Dordrecht.

Rienstra, S. (2003). A classification of duct modes based on surface waves. *Wave Motion*, 37(2):119–135.

Rienstra, S. (2006). Impedance models in time domain, including the Extended Helmholtz Resonator Model. In *12th AIAA/CEAS Aeroacoustics Conference*, Cambridge, MA. AIAA -2006-2686.

Rienstra, S. and Darau, M. (2011). Boundary layer thickness effects of the hydrodynamic instability along an impedance wall. *Journal of Fluid Mechanics*, 671:559–573.

Rienstra, S. and Hirschberg, A. (1992-2004-2015). An introduction to acoustics. Technical Report IWDE 92-06, Technische Universiteit Eindhoven. http://www.win.tue.nl/∼sjoerdr/papers/boek.pdf.

Rienstra, S. and Tester, B. (2008). An analytic Green's function for a lined circular duct containing uniform mean flow. *Journal of Sound and Vibration*, 317:994–1016.

Rienstra, S. and Vilenski, G. (2008). Spatial instability of boundary layer along impedance wall. In *14th AIAA/CEAS Aeroacoustics Conference*, Vancouver, Canada. AIAA -2008-2932.

Schulten, J. (1993). *Sound Generation by Ducted Fans and Propellers as a Lifting Surface Problem*. PhD thesis, University of Twente, Enschede, The Netherlands. ISBN 90-9005714-5.

Smith, M. (1989). *Aircraft Noise*. Cambridge University Press, Cambridge.

Tyler, J. and Sofrin, T. (1962). Axial flow compressor noise studies. *Transactions of the Society of Automotive Engineers*, 70:309–332.

Vilenski, G. and Rienstra, S. (2007). On hydrodynamic and acoustic modes in a ducted shear flow with wall lining. *Journal of Fluid Mechanics*, 583:45–70.

Watson, G. (1944). *A Treatise on the Theory of Bessel Functions*. Cambridge University Press, London, 2nd edition.

Weinstein, L. (1974). *The Theory of Diffraction and the Factorization Method*. Golem Press, Boulder, Colorado.

Wu, C. (1973). Variational and iterative methods for waveguides and arrays. In Mittra, R., editor, *Computer Techniques for Electromagnetics (chapter 5)*, pages 266–304. Pergamon Press, Oxford.

A Appendix

A.1 Bessel Functions

The Bessel equation for integer m (which results naturally if we study the eigenvalue problem $\nabla^2\phi = -\alpha^2\phi$ of the Laplace operator in polar coordinates)

$$y'' + \frac{1}{x}y' + \Big(1 - \frac{m^2}{x^2}\Big)y = 0 \tag{130}$$

has two independent solutions (Watson, 1944; Abramowitz and Stegun, 1964; Erdelyi et al., 1953; Gradshteyn and Ryzhik, 1994; Luke, 1969). Standardized forms are

$$J_m(x),\ m\text{-th order ordinary Bessel function of the 1st kind,} \tag{131a}$$

$$Y_m(x),\ m\text{-th order ordinary Bessel function of the 2nd kind.} \tag{131b}$$

related by the Wronskian

$$J_m(x)Y'_m(x) - Y_m(x)J'_m(x) = \frac{2}{\pi x}. \tag{132}$$

Bessel functions of imaginary argument give rise to modified Bessel functions. A standardised modified Bessel function of the 1st kind is

$$I_m(x) = (-\mathrm{i})^m J_m(\mathrm{i}x) \tag{133}$$

J_m is regular and Y_m is singular in $x = 0$. Mainly relevant for hollow (non annular) ducts is J_m (see figure 25). J_m behaves oscillatory slowly decaying and I_m exponentially

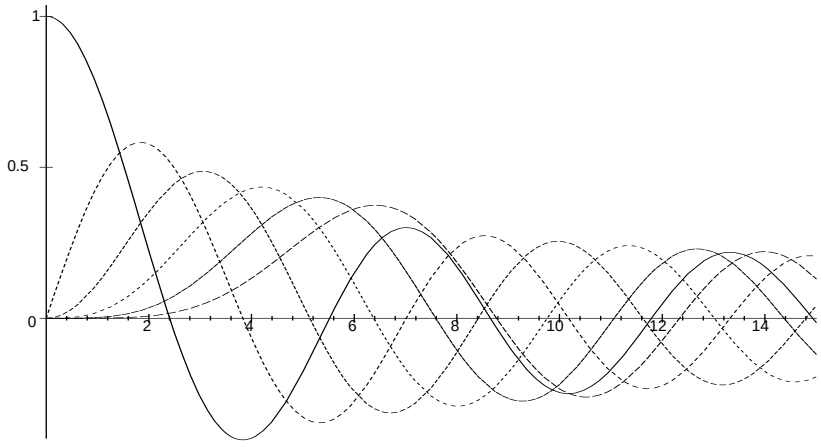

Figure 25: Bessel function $J_m(x)$ for $m = 0, \ldots, 5$.

increasing. $J_m(x)$ and $J'_m(x)$ have an infinite number of real zeros (Table 1), all of which are simple with the possible exception of $x = 0$. The μ-th positive ($\neq 0$) zeros are denoted by $j_{m\mu}$ and $j'_{m\mu}$ respectively, except that $x = 0$ is counted as the first zero of J'_0: $j'_{01} = 0$. It follows that $j'_{0,\mu} = j_{1,\mu-1}$. In general it is true that $j'_{m1} \geqslant m$.

μ \ m	0	1	2	3	4	5	6	7	8	9	10
1	0.0000	1.8412	3.0542	4.2012	5.3176	6.4156	7.5013	8.5778	9.6474	10.711	11.771
2	3.8317	5.3314	6.7061	8.0152	9.2824	10.520	11.735	12.932	14.116	15.287	16.448
3	7.0156	8.5363	9.9695	11.346	12.682	13.987	15.268	16.529	17.774	19.005	20.223
4	10.173	11.706	13.170	14.586	15.964	17.313	18.637	19.942	21.229	22.501	23.761

Table 1: Zero's of $J'_m(x)$

Symmetry relations are

$$J_m(-x) = J_{-m}(x) = (-1)^m J_m(x) \tag{134}$$

Asymptotic behaviour for $x \to 0$:

$$J_m(x) \simeq \frac{(\frac{1}{2}x)^m}{m!} \tag{135}$$

Asymptotic behaviour for $|x| \to \infty$ and m fixed:

$$J_m(x) \simeq \frac{\cos(x - \frac{1}{2}m\pi - \frac{1}{4}\pi)}{\sqrt{\frac{1}{2}\pi x}}, \quad J'_m(x) \simeq -\frac{\sin(x - \frac{1}{2}m\pi - \frac{1}{4}\pi)}{\sqrt{\frac{1}{2}\pi x}} \tag{136}$$

yielding

$$j_{m\mu} \simeq (\mu + \tfrac{1}{2}m - \tfrac{1}{4})\pi, \qquad j'_{m\mu} \simeq (\mu + \tfrac{1}{2}m - \tfrac{3}{4})\pi \quad \text{for} \quad \mu \to \infty \tag{137}$$

Asymptotic behaviour for $m \to \infty$:

$$J_m(x) \simeq \frac{1}{\sqrt{2\pi m}}\Big(\frac{ex}{2m}\Big)^m \tag{138}$$

Important recurrence relations are

$$J_{m-1}(x) + J_{m+1}(x) = 2\frac{m}{x}J_m(x) \tag{139}$$

$$J_{m-1}(x) - J_{m+1}(x) = 2J'_m(x) \tag{140}$$

In particular:

$$J'_0(x) = -J_1(x) \tag{141}$$

Relations involving integrals:

$$\int\Big((\alpha^2 - \beta^2)x - \frac{m^2 - n^2}{x}\Big)J_m(\alpha x)J_n(\beta x)\,\mathrm{d}x = \beta x J'_n(\beta x)J_m(\alpha x) - \alpha x J'_m(\alpha x)J_n(\beta x) \tag{142}$$

$$2\int \alpha^2 x J_m(\alpha x)^2\,\mathrm{d}x = (\alpha^2 x^2 - m^2)J_m(\alpha x)^2 + \alpha^2 x^2 J'_m(\alpha x)^2$$

A.2 An Important Complex Square Root

The following square root plays an important role.

$$\zeta(z) = \sqrt{1 - z^2} \qquad \mathrm{Im}(\zeta) \leqslant 0, \qquad \zeta(0) = 1. \tag{143}$$

The sign choice is made such that always $\mathrm{Im}(\zeta) \leqslant 0$. This implies that the branch cuts are located right along the curves where $\mathrm{Im}(\zeta) = 0$, i.e. along the imaginary axis, and the real interval $|z| \leqslant 1$. For definiteness the branch cuts are included in the domain of definition as the limits from the $\mathrm{Re}\,\zeta > 0$ side. See figure 26. If we take care along the branch cuts, where $\mathrm{sign}(\mathrm{Im}\,\zeta)$ is not defined, a simple[12] way to determine ζ is

$$\zeta(z) = -\,\mathrm{sign}\left(\mathrm{Im}\,\sqrt{1 - z^2}\right)\sqrt{1 - z^2} \tag{144}$$

Note that $\zeta(z) \simeq -\mathrm{i}\,z\,\mathrm{sign}(\mathrm{Re}\,z)$ if $|z| \gg 1$,

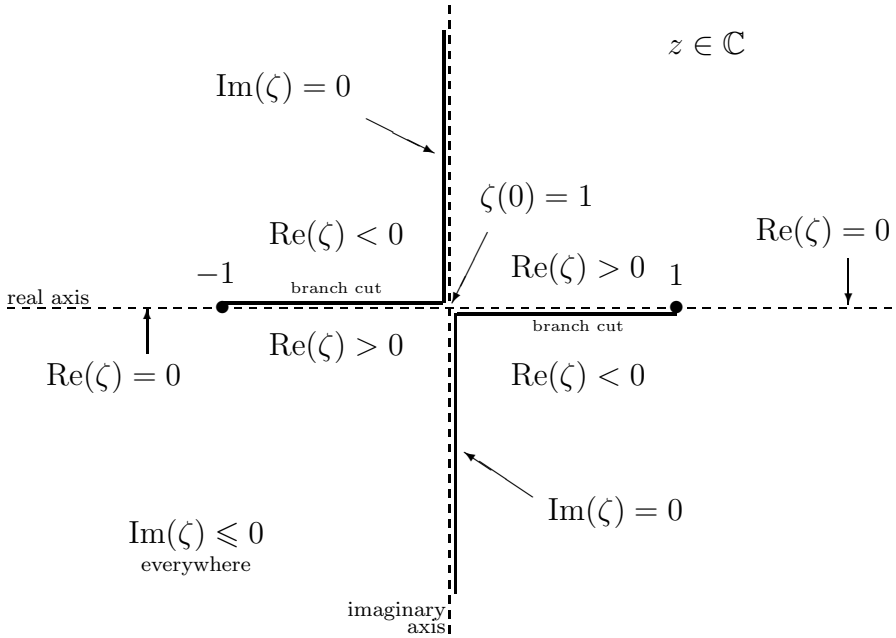

Figure 26: Branch cuts and signs of $\zeta(z) = \sqrt{1 - z^2}$ in complex z-plane.

[12]Note added 2018-08-14: an even simpler form is $\zeta(z) = -\mathrm{i}\sqrt{z^2 - 1}$ with $\sqrt{\cdot}$ the principal value square root. This is even correct along the branch cuts if the usual convention of $\sqrt{-1} = \mathrm{i}$ is adopted.

A.3 Myers' Energy Corollary

When the equations for conservation of mass and momentum and the general energy conservation law for fluid motion are expanded to quadratic order, this 2nd order energy may be reduced to the following conservation law for perturbation energy density E, energy flux $\boldsymbol{I}$, and dissipation $\mathcal{D}$

$$\frac{\partial E}{\partial t} + \nabla\cdot\boldsymbol{I} = -\mathcal{D} \tag{145}$$

with

$$E = \frac{{p'}^2}{2\rho_0 c_0^2} + \frac{1}{2}\rho_0|\boldsymbol{v}'|^2 + \rho'\boldsymbol{v}_0\cdot\boldsymbol{v}' + \frac{\rho_0 T_0 {s'}^2}{2C_p}, \tag{146a}$$

$$\boldsymbol{I} = (\rho_0\boldsymbol{v}' + \rho'\boldsymbol{v}_0)\left(\frac{p'}{\rho_0} + \boldsymbol{v}_0\cdot\boldsymbol{v}'\right) + \rho_0\boldsymbol{v}_0 T' s', \tag{146b}$$

$$\mathcal{D} = -\rho_0\boldsymbol{v}_0\cdot(\boldsymbol{\omega}'\times\boldsymbol{v}') - \rho'\boldsymbol{v}'\cdot(\boldsymbol{\omega}_0\times\boldsymbol{v}_0) + s'(\rho_0\boldsymbol{v}' + \rho'\boldsymbol{v}_0)\cdot\nabla T_0 - s'\rho_0\boldsymbol{v}_0\cdot\nabla T', \tag{146c}$$

as shown by Myers (1991). Mean flow pressure and its perturbation are denoted by p_0 and p', density by ρ_0 and ρ', velocity by $\boldsymbol{v}_0$ and $\boldsymbol{v}'$, sound speed by c_0, temperature by T_0 and T', entropy by s_0 and s', and vorticity by $\boldsymbol{\omega}_0 = \nabla\times\boldsymbol{v}_0$ and $\boldsymbol{\omega}' = \nabla\times\boldsymbol{v}'$.

Note that these equations only contain mean flow and first order perturbation terms. Consequently, this conservation law is exactly valid for small linear disturbances ($p', \boldsymbol{v}'$, etc.) of a mean flow ($p_0, \boldsymbol{v}_0$, etc.).

The perturbation energy defined by E and $\boldsymbol{I}$ is *not* conserved, unless $\mathcal{D} = 0$, for example with irrotational and isentropic flow, or a uniform medium without mean flow.

Taking the time average of (145) for time harmonic perturbations yields

$$\nabla\cdot\langle\boldsymbol{I}\rangle = -\langle\mathcal{D}\rangle. \tag{147}$$

The acoustic power through a surface $\mathcal{A}$ with normal $\boldsymbol{n}$ is

$$\mathcal{P} = \int_{\mathcal{A}}\langle\boldsymbol{I}\cdot\boldsymbol{n}\rangle\,\mathrm{d}\sigma. \tag{148}$$

By taking the volume integral of (147) over a volume $\mathcal{V}$ with boundary $\partial\mathcal{V}$ and applying the divergence theorem, we find

$$\int_{\partial\mathcal{V}}\langle\boldsymbol{I}\cdot\boldsymbol{n}\rangle\,\mathrm{d}\sigma + \int_{\mathcal{V}}\langle\mathcal{D}\rangle\,\mathrm{d}\boldsymbol{x} = 0. \tag{149}$$